Draft version December 3, 2022
Typeset using LaTeX default style in AASTeX631

Bosonic Dark Matter Admixed White Dwarfs and Variable Scattering Length*

C. N. Chu[1,2]

[1]Supervised by Prof. M. C. Chu
[2]Department of Physics, Faculty of Science
The Chinese University of Hong Kong
Shatin, N.T., Hong Kong
China

ABSTRACT

Deviations of observable white dwarfs and recent theory of allowed white dwarfs urges explanations of their existences. Dark matter (DM), with unknown properties, is a promising portal to account for this phenomenon. Fermionic and bosonic DMs are correspondingly admixed to white dwarfs and the properties from these admixtures are studied. Super-Chandrasekhar white dwarfs and small mass large radius white dwarfs are found to be possibly formed with the admixed bosonic dark matter (BDM) and they are stable to exist, showing that admixing BDM can potentially solve the existence problem of white dwarfs with radius $R_n \leq 0.013\ R_\odot$. Variable scattering length of the BDM in a white dwarf (WD) is also studied and results illustrate that WDs are stable even with different repulsive interactions between BDM in different parts of the WD. This is beneficial for further studies on a bosenova (BN) of a bosonic dark matter admixed white dwarf (BDAWD), and suggests that this can only be achieved by an attractive interaction somewhere in the WD.

Keywords: Bosonic Dark Matter — White Dwarf — Variable Scattering Length — Bosenova

1. INTRODUCTION

It is widely accepted that DM contributes to around one-fourth of the energy budget of the whole universe Peter (2012). DM can be implemented to explain the galactic rotation curves and a lot more beyonds D'Amico et al. (2009). With the most successful DM model, ΛCDM model, which states that the DM particles should be non-relativstic, one can explain originally unanticipated observations, including the cosmic microwave background anomalies D'Amico et al. (2009). Currently, weakly interacting massive particle (WIMP) is the most possible candidate among all the others as it is the most powerful one in explaining different phenomena D'Amico et al. (2009).

Despite researches on DM had been carrying out for decades, with experiments set up to detect them underground, physicists have no consensus on the intrinsic properties of DM yet. As defined, DM should not be interacting with normal matter (NM) (any kind of matter one can see and touch right now, this report will stick to this term), except through gravity, or some more unknown interactions. Therefore, a DM particle should have no electric charge D'Amico et al. (2009).

Besides electric charge, one have no clues on the mass of the particles nor their spins, not to mention whether or not DM is actually another family of undetectable elementary particles. Thus, it is very interesting to study the properties of the particles and to constrain the possible ranges of the values.

One possible way to investigate DM is by WDs. WDs are well-understood (for NM) and there is a maximum mass limit for it to exist, which is the Chandrasekhar limit, approximately 1.44 $M_\odot$. Once the total mass of the WD

* Submitted on December, 3rd, 2022

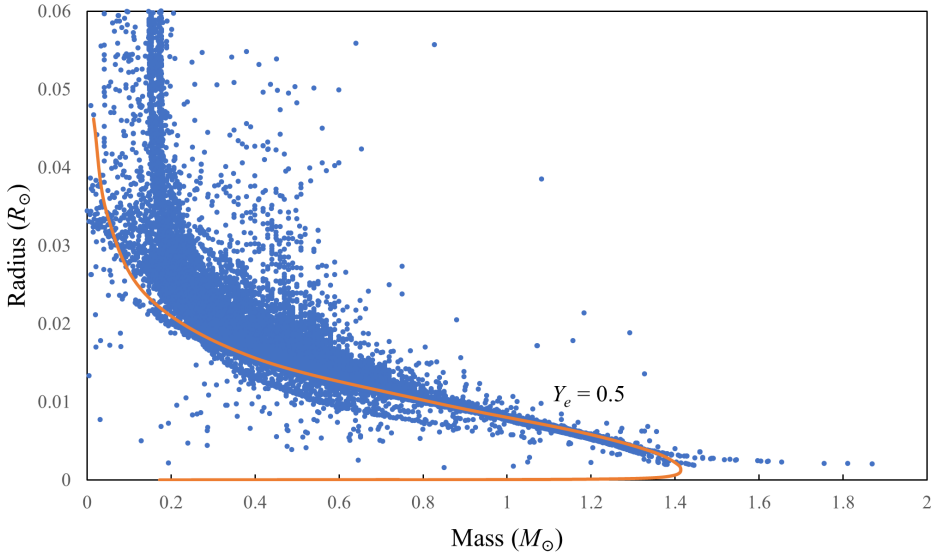

Figure 1. Radius of WDs plotted against total mass (M-R relation) is plotted from the Montreal database as blue scattered data points in the above plot Dufour et al. (2017). The orange line is the M-R relation for the NMWDs with general relativistic modifications considered, at electron ratio $Y_e = 0.5$. The normally allowed WDs are only in a narrow band below the orange curve. This is obviously not in line with our observations where large radius WDs, super-Chandrasekhar WDs ($M > 1.4\ M_\odot$ and some small mass small radius WDs can be seen.

exceeds it, it becomes a Type Ia Supernova (SN). Shown in Figure 1, is the radius of WDs against their total masses detected (M-R relation), got from the Montreal database Dufour et al. (2017). However, one can actually see some super-Chandrasekhar WDs ($M_t > 1.44 M_\odot$), which require explanations.

More than that, one would expect the centre of WDs to consist of carbon or even heavier elements, like iron, but no more further, as iron is the most bounded element. By considering the electron ratios Y_e for both carbon or iron-centred stars, one can find the allowed maximum mass and the corresponding radii for the WDs. These allowed WDs show a narrow band in the M-R relation, which is the classically allowed M-R relation for hydrostatic WDs. Interestingly, there are also WDs with too large or too small radii, they are not really outliers, but there are many of them, so this urges astrophysicists to propose models to unmask the underlying physics.

It is quite reasonable that WDs are rotating along their own axes, and this may account for a slightly larger radius with the centrifugal forces considered in the star reference frame. So the rotation speed can be one of the parameters leading for larger radii WDs. But for smaller radii WDs, this framework does not work.

As mentioned, DM is widely accepted to be existing with a large amount, physicists admix DM into WDs and try to reproduce the WDs detected. While there are no clues what are the spins of DM, they may be fermionic or bosonic in nature. Fermionic dark matter (FDM) had been widely investigated and it can surely provide more gravitational attraction to form denser stars. FDM should obey Pauli's Exclusion Principle, as they are also fermions, and degenerate pressure is expected, so FDM provides gravitational pull and repulsive pressure.

Besides FDM, which is a DM candidate, it may be even more interesting to study BDM as they are not restricted by Pauli's Exclusion Principle. BDM may exist in a form of Bose-Einstein Condensate (BEC) in the star, and they can exhibit both attractive or repulsive interactions, which provide much more dynamical activities to be observed. So it is a kind of model beyond FDM, as it should be able to reproduce the results using FDM, and allow us to produce much more different stars at the same time. The interaction may not be restricted to a specific attractive or repulsive one, as it can be changed by external factors and is model-dependent.

This concept actually arises from BN, which refers to a BEC that experience a change in their interactions, becoming attractive instead of repulsive and cause the BEC to collapse Kagan et al. (1997). Then it rebounds and explode Santos & Shlyapnikov (2002), similar to a SN. Therefore, admixing BDM into a WD and form a BDAWD may give us something similar to BN, which may lead us to new physics. Thus it is interesting to be investigated.

2. METHODOLOGY

To study BDAWDs, the physics in an ordinary WD (NMWD) without any DM admixed should first be studied as a basic model. After mastering the basics, one can then add some components to make the simple model complicated.

2.1. *Newtonian Ordinary White Dwarfs*

In order to set up the set of governing equations for a NMWD, hydrostatic equilibrium is first assumed, and the equations of states (EOS) follows, so that a hydrostatic WD can be produced.

Regarding a regular WD, it is the electron degeneracy pressure balancing the gravitational force of the enclosed mass. For the gravitational force on a unit volume of matter ρ, which is also the mass density, it is given by the Newtonian law of gravity

$$F_g = -\frac{GM}{r^2}\rho, \tag{1}$$

where G is the universal gravitational constant, M is the enclosed mass of a certain radius, which is a function of radius and r is the radius. As density $\rho(r)$ is a function of radius, the enclosed mass $M(r)$, to be exact, is therefore $M(r) = 4\pi \int_0^r \rho(r')r'^2 dr'$. Equivalently, the differential enclosed mass $M(r)$ with different radii r can be written as

$$\frac{dM}{dr} = 4\pi r^2 \rho. \tag{2}$$

Note that in this framework, WDs are assumed to be spherically symmetric and it is actually simulating only in the radial direction.

While the electron degeneracy pressure gradient force and the gravitational force balance each other in the hydrostatic equilibrium case, one can write the equation as

$$\frac{dP}{dr} = -\frac{GM}{r^2}\rho. \tag{3}$$

Then, the form of electron degeneracy pressure should be known in order to deduce dP/dr in the left hand side of Eq. (3).

In a WD, there are heavy nuclei and electrons, just like the ordinary stars. As a WD is quite dense, the electron degeneracy pressure dominates and support the star. We can therefore assume the electrons as a free Fermi electron gas and they are no more bounded by any individual nucleus.

To formulate the degeneracy pressure P, one can start with the mass density of electrons, or similarly the number density of it. This is because when there are more electrons in the same packed region, they are competing to occupy the lowest energy states. Due to Pauli's Exclusion Principle for fermions, electrons have to gain energy to occupy higher and higher energy states, which is getting harder for them to do so. Thus the more electrons packed in the same space, the stronger electron degeneracy pressure is expected. Note that the number density n of electrons is related to the mass density ρ by

$$n = Y_e \frac{\rho}{m_p}, \tag{4}$$

where Y_e is the number of electron per nucleon, the electron ratio and m_p is the proton mass (assuming proton and neutron weigh the same). Therefore, for different elements dominating in a WD, Y_e should be different. Normally, the stellar nuclei may be carbon or iron, as they are stable enough to halt further fusion. Iron is the case when the WD

is heavy enough to fuse elements to it, which is the most stable element, due to its high binding energy per nucleon. And WDs can no more gain energy from binding it further. For the nuclei to be ^{12}C, $Y_e = 6/12 = 1/2$; while for the nuclei to be ^{56}Fe, $Y_e = 26/56 = 0.464$.

Note that in this report, reduced planck constant $\hbar$ and speed of light in vacuum c are put as 1, unless written explicitly.

In a compact star, fermions behave as an ideal Fermi gas. Consider the free Fermi electron gas in a large volume V with N electrons as a quantum problem: particle-in-a-box, one can think that there are standing waves inside a specific region. In each dimension, the solution is $\sin(n\pi x/L)$. The fermions in an ideal Fermi gas model try to occupy the lowest energy plane-wave states, with their momenta p are smaller than p_f, Fermi momentum, and all the way up to it. Including also the two-folded spin degeneracy for electrons, one can get the total number of electrons by

$$N = 2V \int_0^{p_f} \frac{d^3p}{(2\pi)^3}, \tag{5}$$

and the total energy to be

$$E = 2V \int_0^{p_f} \frac{d^3p}{(2\pi)^3}(p^2 + m_e^2)^{1/2}, \tag{6}$$

which is from energy-momentum relation: $E^2 = p^2 + m^2$.

Throughout the project, it is not trivial to take care of the total energy and total number of particle, a rather practical way would be to keep track of the number density n and the energy density E/V. Their expressions will be a slight amendment correspondingly from Eqs. (5) and (6). They are given by

$$n = 2 \int_0^{p_f} \frac{d^3p}{(2\pi)^3}; \tag{7}$$

$$\frac{E}{V} = 2 \int_0^{p_f} \frac{d^3p}{(2\pi)^3}(p^2 + m_e^2)^{1/2}. \tag{8}$$

In fact, after computing the integration explicitly, one can get the form of energy density as

$$\frac{E}{V} = n_0 m_e x^3 \epsilon(x), \tag{9}$$

where the scale number density n_0, definitions of x and $\epsilon(x)$ are given by

$$n_0 = \frac{m_e^3}{3\pi^2} = 5.89 \times 10^{29} cm^{-3}; \tag{10}$$

$$x \equiv \frac{p_f}{m_e} = \left(\frac{n}{n_0}\right)^{1/3}; \tag{11}$$

$$\epsilon(x) = \frac{3}{8x^3}[x(1+2x^2)(1+x^2)^{1/2} - \log[x + (1+x^2)^{1/2}]]. \tag{12}$$

As matters in WD can be treated as nearly a perfect fluid, one can use the first law of thermodynamics to deduce the pressure by $dE = TdS - PdV + \mu dN$. Therefore, at fixed number of particles, pressure P can be found by

$$P = -\frac{\partial E}{\partial V} = -\frac{\partial E}{\partial x}\frac{\partial x}{\partial V}. \tag{13}$$

Using Eq. (11), one can deduce that $\frac{\partial x}{\partial V} = -\frac{x}{3V}$ and thus we can get the analytical form of pressure as

$$P = \frac{1}{3} n_0 m_e x^4 \epsilon' \quad ; \quad \epsilon' = \frac{d\epsilon}{dx}. \tag{14}$$

Note that in Eq. (11), we showed that x is related to the scale number density n_0, equivalently, by multiplying the proton mass m_p, we can also relate x with the mass density ρ by

$$x = \left(\frac{n}{n_0}\right)^{1/3} = \left(\frac{\rho}{\rho_0}\right)^{1/3} = \overline{\rho}^{1/3} \quad ; \quad \rho_0 = \frac{m_p n_0}{Y_e} = 9.79 \times 10^5 \ Y_e^{-1} \text{g cm}^{-3}. \tag{15}$$

Physically, the scale mass density ρ_0 is the mass density of NM when electron number density is n_0.

In fact, Eq. (3) can be rewritten using chain rule, and the derivation is:

$$\frac{dP}{dr} = \left(\frac{d\rho}{dr}\right)\left(\frac{dP}{d\rho}\right); \tag{16}$$

$$\frac{d\rho}{dr} = \left(\frac{dP}{d\rho}\right)^{-1}\left(\frac{dP}{dr}\right); \tag{17}$$

$$\frac{d\rho}{dr} = -\left(\frac{dP}{d\rho}\right)^{-1}\frac{GM}{r^2}\rho. \tag{18}$$

We can now get the $\frac{dP}{d\rho}$ term as

$$\frac{dP}{d\rho} = \frac{dP}{dx}\frac{dx}{d\rho} = Y_e\frac{m_e}{m_p}\gamma(x), \tag{19}$$

and the function $\gamma(x)$ is defined by

$$\gamma(x) = \frac{1}{9x^2}\frac{d}{dx}(x^4\epsilon') = \frac{x^2}{3(1+x^2)^{1/2}}. \tag{20}$$

Thus we can now combine Eqs. (18) - (20) to get the differential relationship between density ρ and radius r as

$$\frac{d\rho}{dr} = -\frac{1}{Y_e(m_e/m_p)\gamma}\frac{GM}{r^2}\rho. \tag{21}$$

More naturally to implement into the program, we should scale the equations with some scaling constants so that the prefactors of the two governing equations will be 1, and the coding will be easier to handle dimensionless values. We can simply get back what we need by multiplying the correct scales at last. Define

$$r = R_0\overline{r}, \ \rho = \rho_0\overline{\rho}, \ M = M_0\overline{M}. \tag{22}$$

Therefore, with the scaling, Eqs. (2) and (21) become

$$\frac{d\overline{M}}{d\overline{r}} = \left(\frac{4\pi R_0^3\rho_0}{M_0}\right)\overline{r}^2\overline{\rho}; \tag{23}$$

$$\frac{d\overline{\rho}}{d\overline{r}} = -\left(\frac{GM_0}{R_0Y_e(m_e/m_p)}\right)\frac{\overline{M}\overline{\rho}}{\gamma\overline{r}^2}. \tag{24}$$

To make the prefactors to be unity, we can now define scaling radius R_0 and scaling mass M_0 as

$$R_0 = \left[\frac{Y_e(m_e/m_p)}{4\pi G\rho_0}\right]^{1/2} = 7.72 \times 10^8 \ Y_e \text{ cm}; \tag{25}$$

and

$$M_0 = 4\pi R_0^3\rho_0 = 5.67 \times 10^{33} \ Y_e^2 \text{ g}. \tag{26}$$

Then we can now get a set of very nice and neat governing differential equations for $\overline{\rho}$, $\overline{M}$ and $\overline{r}$ of a WD with solely normal matter. The governing equations are

$$\frac{d\overline{M}}{d\overline{r}} = \overline{r}^2\overline{\rho}; \tag{27}$$

$$\frac{d\overline{\rho}}{d\overline{r}} = -\frac{\overline{M}\overline{\rho}}{\gamma\overline{r}^2}. \tag{28}$$

One can then solve the above two equations for different radius and get the profile of a star, which means we can nowbuild a hydrostatic WD in equilibrium.

In fact, a usual description of a star is by a polytropic EOS, which takes the form of

$$P = k\rho^\gamma. \tag{29}$$

γ is different from the one defined in Eq. (20), and this is actually the adiabatic index, sort of related to the degree of freedom of the molecules. For the degenerate electron gas at extreme non-relativistic limit, or equivalently low-density limit, $\gamma = 5/3$; while for extreme relativistic limit, $\gamma = 4/3$. Therefore, for the degenerate electron gas in WDs, normally we expect $4/3 < \gamma < 5/3$.

By using the polytropic EOS, one can easily vary the physics by varying the adiabatic index γ after having the formula relating pressure P and density ρ, providing an easier way to study different physics, maybe unknown one.

2.2. *TOV corrected Ordinary White Dwarfs*

Note that the above derivation is based on Newtonian gravity, which is still a good enough theory for WDs. However, in fact we know that for compact stars, we should start consider the corrections due to general relativity. It is needed to be included for a high mass WD or more compact objects like a neutron star (NS) or a black hole (BH).

Therefore, to be more precise, we can put in the correction terms and it becomes the Tolman-Oppenheimer-Volkoff (TOV) equation Oppenheimer & Volkoff (1939), given as

$$\frac{dP}{dr} = -\frac{GM}{r^2}\rho\left(1+\frac{P}{\rho}\right)\left(1+\frac{4\pi r^3 P}{M}\right)\left(1-\frac{2GM}{r}\right)^{-1}. \tag{30}$$

The first term is basically the Newtonian gravity, and the last three terms are the relativistic corrections. So we can actually replace Eq. (3) by Eq. (30) and get a new set of governing equations. Eq. (27) is still the same as it is not affected. But for Eq. (21), it should now become

$$\frac{d\rho}{dr} = -\frac{1}{Y_e(m_e/m_p)\gamma}\frac{GM}{r^2}\rho\left(1+\frac{P}{\rho}\right)\left(1+\frac{4\pi r^3 P}{M}\right)\left(1-\frac{2GM}{r}\right)^{-1}. \tag{31}$$

By scaling the equation again, and combining constants to simplify or make them unitary, one can at last get the governing equations to be

$$\frac{d\overline{M}}{dr} = \overline{r}^2\overline{\rho}; \tag{32}$$

$$\frac{d\overline{\rho}}{dr} = -\frac{\overline{M}\overline{\rho}}{\gamma\overline{r}^2}\left(1+\frac{1}{3}\frac{Y_e m_e}{m_p}x^4\epsilon'\frac{1}{\overline{\rho}}\right)\left(1+\frac{1}{3}\frac{Y_e m_e}{m_p}x^4\epsilon'\frac{\overline{r}^3}{\overline{M}}\right)\left(1-2\frac{Y_e m_e}{m_p}\frac{\overline{M}}{\overline{r}}\right)^{-1}. \tag{33}$$

Note that when the radius is small, our density can be too large that there might be numerical errors blowing up for $d\overline{\rho}/d\overline{r}$. Therefore, one should take care of it by expanding the equation at high ρ and low r, this should be taken into accounts for all $d\overline{\rho}/d\overline{r}$ at small r. To deal with it, use total mass M at small r is

$$\overline{M} = \frac{\frac{4}{3}\pi R_0^3\overline{r}^3\rho_0\overline{\rho}}{M_0}. \tag{34}$$

The above definition is universal, so both NM and DM take this form for simplification at small r, and surely $\overline{\rho}$ has to be the sum of the two components' densities. This also helps to simplify the equations for small r, but for simplicity and more general cases, the small r case equations will not be put here. They are just some techniques in programming but not related to the underlying physics here.

2.3. *Fermionic Dark Matter Admixed White Dwarfs*

After successfully setting up a WD contianing only NM, we want to see if admixing DM in a WD will affect its properties and whether it can explain all the different M-R distributions in the observations.

As aforementioned, we have no idea on what the DM looks like. Therefore, we will study both fermionic and bosonic dark matters and fermionic comes first, then we will mainly focus on BDM. And the compact star using the upcoming formalism is then a Fermionic Dark Matter Admixed White Dwarf (FDAWD).

Note that subscripts $_d$ refers to dark matter variables; $_n$ for normal matter variables.

Firstly, let us make little amendments to the normal matter governing equations as shown in Eqs. (32) and (33). We should be careful that the total mass in Eq. (32) refers to only the mass of one component, and Eq. (33) refers to the total mass of the two fluids. So with the admixed FDM, the NM governing equations are

$$\frac{d\overline{M_n}}{dr} = \overline{r}^2\overline{\rho_n}; \tag{35}$$

$$\frac{d\overline{\rho_n}}{dr} = -\frac{\overline{M_t}\overline{\rho_n}}{\gamma_n\overline{r}^2}\left(1+\frac{1}{3}\frac{Y_e m_e}{m_p}x_n^4\epsilon_n'\frac{1}{\overline{\rho_n}}\right)\left(1+\frac{1}{3}\frac{Y_e m_e}{m_p}x_n^4\epsilon_n'\frac{\overline{r}^3}{\overline{M_t}}\right)\left(1-2\frac{Y_e m_e}{m_p}\frac{\overline{M_t}}{\overline{r}}\right)^{-1}. \tag{36}$$

Where $\overline{M_t}$ refers to dimensionless scaled total mass:

$$\overline{M_t} = \overline{M_n} + \overline{M_d}. \tag{37}$$

For Eq. (27) for DM, it always stays the same, just the definition of density, and therefore is

$$\frac{d\overline{M_d}}{d\overline{r}} = \overline{r}^2\overline{\rho_d}. \tag{38}$$

But for the differential relationship between ρ_d and r, we have to rederive it.

In this report, we will assume DM contains only one particle but not a family. So the dark matter particle mass will be m_d. Therefore, for DM, we do not have the concept of Y_e, the ratio of electrons to protons. Or we can say $Y_{e,d} = 1$.

Following the derivations as before, one can get the following quantities as

$$x_d = \left(\frac{3\pi^2\rho_d}{m_d^4}\right)^{1/3}; \tag{39}$$

$$\gamma_d(x_d) = \frac{x_d^2}{3(1+x_d)^{1/2}}; \tag{40}$$

$$\epsilon_d = \frac{3}{8x_d^3}\left[x_d(1+2x_d^2)(1+x_d^2)^{1/2} - \log[x_d+(1+x_d^2)^{1/2}]\right]. \tag{41}$$

And most importantly, the governing equation after scaling is

$$\frac{d\overline{\rho_d}}{d\overline{r}} = -\frac{Y_e m_e}{m_p}\frac{\overline{M_t}\overline{\rho_d}}{\gamma_d\overline{r}^2}\left(1+\frac{1}{3}\frac{Y_e m_d^4}{m_p m_e^3}x_d^4\epsilon_d'\frac{1}{\overline{\rho_d}}\right)\left(1+\frac{1}{3}\frac{Y_e m_d^4}{m_p m_e^3}x_d^4\epsilon_d'\frac{\overline{r}^3}{\overline{M_t}}\right)\left(1-\frac{2Y_e m_e}{m_p}\frac{\overline{M_t}}{\overline{r}}\right)^{-1}. \tag{42}$$

Therefore, by using Eqs. (35)-(38) and (42), we can again solve the WD at equilibrium out, but with FDM admixed.

Remember that the above arguments are not restricted to a specific DM particle mass m_d (the only assumption is that there is only one kind of DM particle), so we can actually get try to vary m_d to see different physical pictures.

To match with the observational data, we may get a specific range of allowed DM particle mass m_d. This helps to justify and perform cross-checking with other m_d derived from other physical phenomena. Predictions may even be made based on it.

2.4. *Bosonic Dark Matter Admixed White Dwarfs*

Admixing FDM surely provides a new way to study WDs. But BDM is the one in interest of this report and may possibly provide some new physics to us. So besides FDM admixing into a WD, bosonic formalism are derived and they can be used to compare with FDAWD.

To start with, we need to zoom in to the microscopic world with quantum nature described by the Gross-Pitaevskii equation (GP equation) Chavanis (2020). It describes the self-interacting bosons in BEC, and shows the time evolution of the wave function in the Time-Dependent Schrödinger Equation (TDSE). We take the BEC as the bosonic part (the DM fluid) of the DM admxied compact star. The GP equation is

$$\left(-\frac{\hbar^2}{2m_d}\nabla^2 + m_d\Phi + \frac{4\pi\hbar^2 a_s}{m_d^2}\rho_d\right)\psi = i\hbar\frac{\partial\psi}{\partial t}. \tag{43}$$

Where the variables are BDM BEC wave function ψ, BDM particle mass m_d, BDM self-interaction scattering length a_s, gravitational potential Φ.

Scattering length can be treated as the length scale where bosons see the self-interaction potential important. Therefore, it shows physically the strength of the self-interaction. For a_s goes to 0, it is the non-interacting limit. For a_s to be positive, bosons self-interaction is repulsive. For a_s to be negative, bosons self-interaction is attractive.

Note that the gravitational potential Φ is computed from the Poisson equation as

$$\nabla^2\Phi = 4\pi G(\rho_n + \rho_d). \tag{44}$$

The wave function solution ψ of Eq. (43) is normalized, one can actually compute DM density by $\rho_d = Nm|\psi|^2$.

To get back some fluid dynamics equation as the Newton's Second Law (i.e. $F = ma$) from the GP equation, we can apply the Madelung transformation. So we have the guess solution of wave function ψ to be

$$\psi = Ae^{iS/\hbar}. \tag{45}$$

The A and S above are simply some real functions. Besides the definition of wave function ψ, we also define a vector, the velocity of DM $\overrightarrow{v_d}$ to be

$$\overrightarrow{v_d} = \frac{\nabla S}{m}. \tag{46}$$

After substituting Eqs. (45) and (46) into Eq. (43) and by using vector identities and expansions, grouping real and imaginary parts correspondingly. With messy algebras, one can finally get back two equations. These two equations are hydrodynamics-like, but with a slight modification, which can be seen when comparing with the normal hydrodynamics equations for NM.

The first one can be obtained is simply the conservation of mass, given by

$$\frac{\partial\rho_d}{\partial t} + \nabla\cdot(\rho_d\overrightarrow{v_d}) = 0. \tag{47}$$

The first term refers to the time evolution of DM density at a certain point, while the second one is the advection term of density, or equivalently the mass. So if mass is advected out, then apparently density at that point will decrease.

And the second one can be obtained is simply the conservation of momentum, or equivalently Newton's Second Law, $\overrightarrow{F} = m\overrightarrow{a}$. For sure, this equation is in vector form, so it actually contains three equations here. The conservation of momentum is

$$\frac{\partial\overrightarrow{v_d}}{\partial t} + (\overrightarrow{v_d}\cdot\nabla)\overrightarrow{v_d} = -\frac{1}{\rho_d}\nabla P_d - \nabla\Phi - \frac{1}{m_d}\nabla Q. \tag{48}$$

There are five terms above, the first term on the left hand side is again the time evolution of the DM velocity at

a certain point; while the second term on the left hand side refers to an advection too, but the advection of momentum.

On the right hand side, the first term is a pressure-gradient force term, which is commonly seen in fluid mechanics, and this helps physicists to define the pressure of BDM. So this term shows a force arises from the gradient of the pressure, to balance the pressure. By this, we can then have the definition of pressure of BDM P_d as

$$P_d = \frac{2\pi a_s}{m_d^3}\rho_d^2. \tag{49}$$

For the second term on the right hand side, it is the gradient of the gravitational potential $\nabla\Phi$, which is actually the gravitational force, and remember that the gravitational potential contains the information of both NM and DM, which is the only part allowing NM and DM interact.

For the last term on the right hand side, it is the special part of the BDM as this quantum potential Q is new to the equation. This quantum potential takes the form of potential (multiplied by BDM particle mass m_d). This potential term shows also the self-interaction between BDMs at their quantum natures. The quantum potential is defined by grouping the terms as

$$Q = -\frac{1}{2m_d}\frac{\nabla^2\sqrt{\rho_d}}{\sqrt{\rho_d}}. \tag{50}$$

Note that from Eq. (49), we can again take the form of pressure as polytropic, as suggested by Eq. (29). As a result, one can simply vary the form of k and polytropic index $\gamma = 2$ and get a new simulation model with BDM.

In fact, the NM component has not been mentioned in the above model, but for NM, they follows the normal hydrodynamics equations. Therefore, the hydrodynamics equations for NM are

$$\frac{\partial\rho_n}{\partial t} + \nabla\cdot(\rho_n\overrightarrow{v_n}) = 0; \tag{51}$$

$$\frac{\partial\overrightarrow{v_n}}{\partial t} + (\overrightarrow{v_n}\cdot\nabla)\overrightarrow{v_n} = -\frac{1}{\rho_n}\nabla P_n - \nabla\Phi. \tag{52}$$

For sure, the above equations are also talking about the conservation of mass and momentum for NM. For Eq. (52), it reduces back to the condition that gravitational force is balanced by the pressure gradient force (from the electron degeneracy pressure) when the left hand side is 0. Therefore, to build a star at hydroequilibrium, we can still use our framework discussed before.

In order to build a hydroequilibrium star as before, we can now vary the polytropic index γ to 2 and use to corresponding definition of k. One may question how can we implement the equations when there is the Q-term in Eq. (48) for DM. In fact, we can show, in later parts 4 during analysis, that this term plays a very insignificant role and we can definitely neglect it. So the equations are still sort of symmetric between NM and DM, just with different definition of pressure P.

Therefore, with the different definitions of pressure, our differential relationship between density and radius for DM, Eq. (42), has to be modified. Once again, we have to follow the derivation.

From Eq. (49), we have the definition of pressure P_d in terms of density ρ_d, and we can now get

$$\frac{dP_d}{d\rho_d} = \frac{4\pi a_s}{m_d^3}\rho_d. \tag{53}$$

Putting it back to Eq. (18), we can now have the differential relationship between ρ_d and r as

$$\frac{d\rho_d}{dr} = -\frac{m_d^3}{4\pi a_s}\frac{1}{\rho_d}\frac{GM_t}{r^2}\rho_d \times (\text{TOV corrections}). \tag{54}$$

By scaling using scaling constants and try our best to make the constants unitary, we can observe that a constant (a combination of constant) always involves in the equation. Here we define it as P_0, which takes the same form as the pressure of BDM in Eq. (49), to be

$$P_0 = 2\pi\rho_0 \frac{a_s}{m_d^3}. \tag{55}$$

Note that in the equation, it should actually be a dimensionless constant, so some $\hbar$ and c have to be added back during computation.

With the definition of P_0, we can now have the governing equation to be

$$\frac{d\overline{\rho_d}}{d\overline{r}} = -\frac{Y_e m_e}{m_p}\frac{1}{2P_0}\frac{\overline{M_t}}{\overline{r}^2}\left(1+P_0\overline{\rho_d}\right)\left(1+P_0\frac{\overline{r}^3\overline{\rho_d}^2}{\overline{M_t}}\right)\left(1-2\frac{Y_e m_e}{m_p}\frac{\overline{M_t}}{\overline{r}}\right)^{-1}. \tag{56}$$

Therefore, we finally get all the governing equations to be solved to build the initial condition of a BDAWD, using Eqs. (35) - (38) and (56).

We once have mentioned that the one can use different m_d for FDM to obtain different physics and form different WDs. And it may be used for further predictions.

However, for BDM, one more parameter comes in, which is the BDM self-interaction scattering length a_s. This seems to make the parameter space more complicated, but taking a look at Eq. (56), we can find that a_s is always coupled to m_d^3 in P_0 shown in Eq. (55). This means that a_s/m_d^3 is actually a single parameter. Not each one of them is really important but the combination of it.

To understand it, we should see that the self-interaction scattering length is closely related to the BDM particle mass. For an order of magnitude of change in m_d, three orders of magnitude of change in a_s can compensate it and makes no differences for the physics.

More interestingly, one can consider simply change a_s and fix m_d to study the effect of the whole parameter a_s/m_d^3. This is also equivalent to fix a self-interaction strength and vary the BDM particle mass m_d.

It is a sad story that one may cannot directly determine the allowed mass range m_d from the formalism above, or the BDM self-interaction strength, but only their combined effect. The values of a_s and m_d are required to be solved from other methods, or by more dynamics in WDs to be seen later.

2.5. *Weighted Essentially Non-Oscillatory code*

To analyse hydrodynamics of the stars, Eqs. (51) - (52) are the governing equations for NMWDs; Eqs. (47) - (48) and (51) - (52) are the governing equations for FDAWD and BDAWDs. Surely that to build a star at equilibrium is what we have been discussing for the previous pages. This is possible that we may reveal some interesting effects, after admixing different types of DMs into a WD, and see the change of maximum total mass allowed.

However, no one can tell if the star built is stable or not without letting it evolve with time after building it initially. Therefore, hydrodynamical program is required.

Weighted essentially non-oscillatory (WENO) code is a scheme first proposed in 2001, and is able to handle shocks with high resolutions Shu (2003). It allows us to perform hydrodynamical simulations for a WD, even with DM admixed.

However, one limit is that the code is in Newtonian formalism instead of taking TOV corrections into accounts. So when performing hydrodynamical simulation, one should always check if the initial star built is similar to the one built with TOV modifications. Or simply, to check whether general relativity modifications on gravity are important.

If so, the results from the simulations using WENO are meaningless.

WENO code is used to do simulations on basically all the mentioned stars: NMWDs, FDAWDs and BDAWDs. They are now in Newtonian formalisms.

2.5.1. *WENO: Vibration of Stable White Dwarfs*

Using WENO code, one can, most importantly see how the central densities, equivalently the whole star, is fluctuating periodically. In fact, this refers to the shaking of the star, which is very natural, any slight perturbation in any part of the star may lead to an oscillation.

The most important part is to verify that, the star is a stable one (i.e. the shaking continues for periods and does not show a runaway effect). It is because only the stable ones are able to be observed and likely to be formed in reality, so only those that are stable will exist in our database.

For a stable star generated, we can also add perturbation, such as the initial velocities for each fluid, and see how it evolves. This will be even more promising if a star with a greater initial perturbation stays vibrating for periods, then we may conclude that the star is really stable. This is applicable to all three kinds of WDs for checking the stability.

Different velocity profiles can be added, such as a linear one

$$v = v_0 r, \tag{57}$$

or a logarithmic one

$$v = v_0 \log(r) \tag{58}$$

etc. They may not be really physical at all, but our goal is to make some perturbations to see if the star gets back to its original state. Most importantly is to show the star remains vibrating instead of exploding out. So the form of velocity profiles implemented may not be that important.

2.5.2. *WENO: Sedov Test*

Another main hydrodynamical simulation to be done by WENO is the Sedov test, which means basically injecting an enormous amount of energy to the NM and the star will then explode. In WENO, the injection of energy is in the form of temperature, or internal energy equivalently. Then one can see the star explodes and the total enclosed mass eventually decreases. We had carried out several Sedov tests on NMWD but did not analyse the data from it in detail, as our project goal is not really on it.

By analysing the total mass evolution curves, or other profiles including densities or velocities, we may find whether the results are in line with our expectations. It is likely that the explosion of NM will affect DM, but as DMs interact weakly, only by gravity (for FDM; self-interaction is another for BDM), one may see totally different results from the Sedov tests for FDAWDs and BDAWDs. It worths investigations and is a possible further study.

Further studies can also be made once a difference in Sedov test results can be seen, that the energy injection profile can be in an expression of ρ_d to some powers. The index of ρ_d determines whether the energy comes from a DM decay (power = 1) or a DM-DM annihilation (power = 2) or even a NM-DM interaction and so on. However, in view of the limited time, we will not discuss it in later parts.

2.5.3. *Variable Scattering Length a_s for Bosonic Dark Matter Admixed White Dwarfs*

A possible final goal of this project is to study BNe, conventionally means that a BEC is experiencing a change in self-interaction from repulsive to attractive, then causes the BEC to explode and release energy, and rebound. The change of self-scattering interaction can be caused by some unknown mechanisms, especially for BECs formed by BDMs.

Here we are interested in an enormous BN, as the BDM in a BDAWD. In order to deal with a BN and study its dynamics, a BDAWD with variable scattering length a_s may be the portal. Then we may get to BN by changing the interactive force using the variable a_s.

One way to build a BDAWD with variable a_s is that we assume a_s depends on DM density, possibly in a form of

$$a_s = a_{s,crit}\left(1 + \eta\frac{\rho_{d,crit} - \rho_d}{\rho_{d,crit}}\right). \tag{59}$$

Where $a_{s,crit}$ is the dominant a_s which is not depending on density; η is a new dimensionless parameter to show the dependence of BDM density; $\rho_{d,crit}$ is the critical density of BDM, which can be set to any value, and is at where the interaction strength be exactly $a_{s,crit}$.

As a_s refers to the self-interaction strength, it is highly possible that the interaction depends on its own density. Thus our first try is to use Eq. (59) as an expression of a_s.

Besides the above Eq. (59) as the expression of the varying a_s, some more expressions can be used too, maybe an exponential one, squared density one, sinusoidal one. But they can be the further studies to be conducted, here we are sticking to Eq. (59) first as this linear relation is the most simplified model for variable a_s.

Another motivation of this varying a_s is that there will usually be tiny fluctuations or a possible range for any physical parameter, maybe the self-scattering strength or even the DM particle mass. Therefore, varying a_s (or equivalently varying m_d) can also be used to study this uncertainty problem, by simply setting the density dependence η to be small, maybe using other expressions as well.

After successfully implemented Eq. (59), we can put BDAWDs in the WENO code again to see how they evolve. It may cause really a BN, or still a stable BDAWD, it is therefore interesting to be investigated.

Note that in later sections, one can see that whenever a_s has become negative, meaning an attractive self-interaction, causes the star to collapse to a BH. Therefore, it is also possible to see the effect if only a tiny part, maybe the outermost or the innermost part of the star suddenly experiences an attractive self-interaction while the other are still repulsive. This may causes unknown dynamics or vibration or even explosion of the BDAWD.

3. RESULTS AND ANALYSIS

Results from different models will be discussed and different sections below refer to the usage of the EOS for corresponding systems.

3.1. *Newtonian Ordinary White Dwarfs*

For a NMWD, we can change the electron ratio Y_e to see how the M-R relation looks like. Shown in Figure 2 is the M-R relation plotted for different Y_e.

From Figure 2, we can easily deduce that for a larger electron ratio Y_e, one can have a larger Chandrasekhar limit M_{Ch}, and the allowed distribution of WDs M-R relation is different. But it is important to note that, both $Y_e = 0.6$ and 0.4 cases are basically unphysical. For a WD to exist, they should usually have a core with element carbon, or at most iron. So the allowed Y_e should possibly range from 0.464 to 0.5. The above plot is simply for visualising the effect of Y_e.

Therefore, we can now know that under the Newtonian gravity framework, we will have the maximum allowed mass of WDs with iron core to be slightly smaller than that of a carbon core. And the maximum allowed total mass of a NMWD with carbon core is $1.445M_\odot$. This is what we refer to as M_{Ch} under the Newtonian framework.

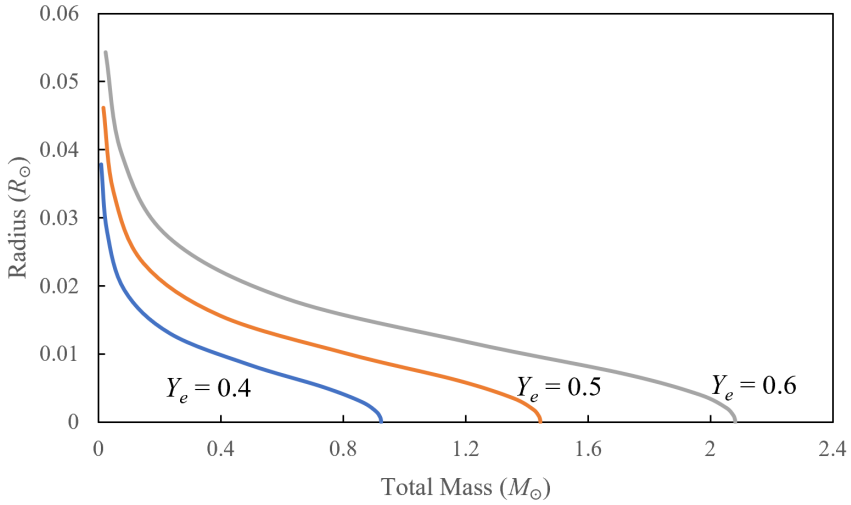

Figure 2. Radius of a NMWD R against the total enclosed mass M with different Y_e. The blue line refers to the M-R relation of $Y_e = 0.4$; the orange line refers to that of $Y_e = 0.5$; the grey line refers to that of $Y_e = 0.6$. This is mainly for showing the trend when Y_e increases, the M-R relation curve shifts rightward. The actual allowed band of M-R relation is a small band right below the orange line, considering that usually we have $0.464 < Y_e < 0.5$.

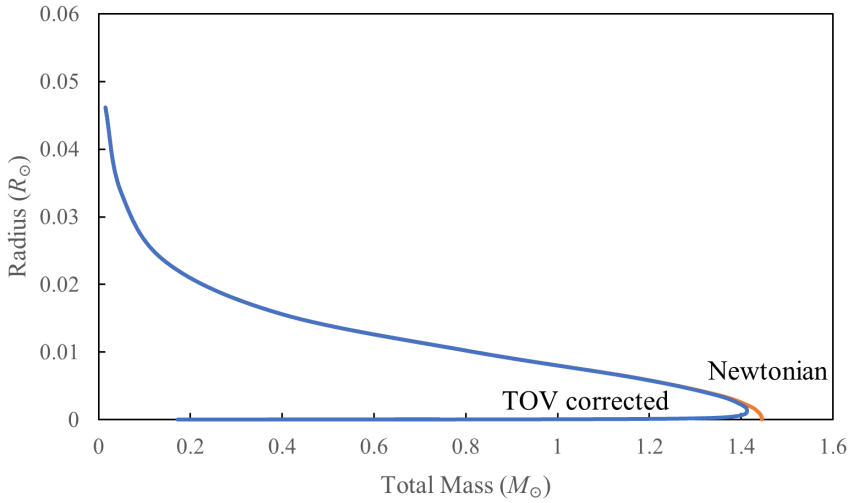

Figure 3. Radius of a NMWD R against the total enclosed mass M as a M-R relationship. The orange line still stands for the relation at $Y_e = 0.5$ in Newtonian framework; and the blue line stands for that in TOV corrected framework. There are basically no differences between the two M-R relation for smaller masses WDs, but the line deviates at larger masses. This shows that TOV corrections help to suppress M_{Ch}.

3.2. *TOV corrected Ordinary White Dwarfs*

Then we can now see how general relativity tells M_{Ch} to be suppressed by a bit. In Figure 3, M-R relation is plotted for both Newtonian and TOV frameworks, with the same electron ratio $Y_e = 0.5$. Note that all the upcoming discussions and the results produced are in the ratio $Y_e = 0.5$.

Obviously one can see that for the upper part (lower mass) cases, the lines overlap, meaning that the TOV corrections basically has no effect on the small mass WDs or equivalently a lower central density WD. They are only affecting the M-R relation for WDs with larger masses, when approaching the Chandrasekhar limit. In this way, M_{Ch}

is suppressed to $1.412M_{\odot}$.

Moreover, the bending of the M-R relation curve shows that the larger masses WDs are unstable, meaning that for a WD with even higher central density, it may not be formed. This is because when we are accreting matters, we always accrete from smaller total mass. Then when we accrete more, it reaches M_{Ch} and became a SN, so higher central density WDs are impossible.

3.3. *WENO: Normal Matter White Dwarfs*

After successfully constructed the M-R relations, we can get a taste of their hydrodynamical stability with WENO code. As aforementioned, WENO uses Newtonian gravity so we cannot really check whether the WDs with high central densities can be formed (or are stable). But we can still have an idea of how a star is vibrating.

For easier computation, the graphs generated by the WENO code are in the code unit, with a time span of 10^6 units refer to around 5 seconds in the real world. Here we plotted the graph from a NMWD with the central density $\rho_c = 10^{10}$ g cm^{-3}.

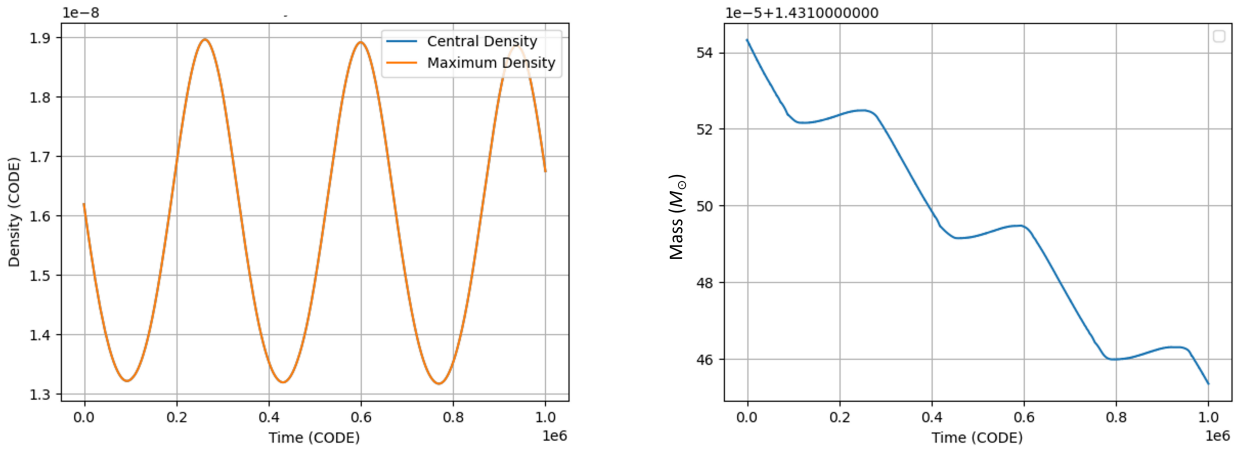

Figure 4. (Left) Time evolution of central density of NM ρ_c for a NMWD. (Right) Time evolution of total mass M_n in $M_\odot$ for a NMWD. They are both undergoing, basically, a simple harmonic motion, showing that it is a stable WD.

From the graphs in Figure 4, we can really see how a WD oscillate, especially from the left graph. It basically looks like a simple harmonic motion (SHM) with a well defined period T. Plotting the central density is just a specific case, one can also plot any point and we should get a similar graph with the same shape. But typically, we can see that the WD is able to get back to its original phase with several cycles of oscillations, showing that it is stable.

You may wonder the right panel seems to show that there is a mass loss of the WD, but note that the y-axis in the plot is the mass in solar mass $M_\odot$, and the deviation is actually in the order of 10^{-4} $M_\odot$, a lot smaller than its value, so it can simply be treated as some numerical errors and we are still having a stable WD.

Regarding the SHM, one can actually tell its oscillation period and do a Fast Fourier Transform (FFT) to get its oscillation frequency. The frequency graph of the above NMWD as an example is plotted.

From Figure 5, we can see that there are two peaks (or maybe a very minor third peak), the lowest frequency one is the fundamental or dominated one, in line with the oscillation we can see in the left graph in Figure 4. Those higher frequencies are just the harmonics of the fundamental mode. This oscillation period is probably the normal mode of the WD, and the normal mode varies from WD to WD with different central densities, or equivalently the density

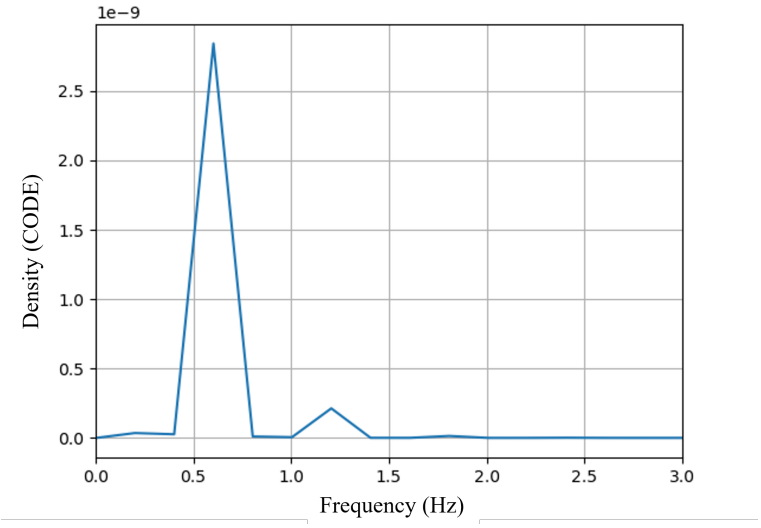

Figure 5. FFT plot for a NMWD with amplitude of central density against frequency. This shows the evidence of the WD is undergoing a SHM, with higher resonances too.

profiles.

Actually one can prove whether the above frequency is reasonable or not, using an approximation. Graphically, one can compare the results. For the above WD, the FFT shows that the dominant frequency is around 0.6 Hz. Using the oscillation in Figure 4, we can see that graphically, the oscillation period is around 3.4×10^5 code time units, referring to approximately $1.6747s$ for a period. Therefore, a frequency of 0.59712 Hz, in line with our FFT graph.

Mathematically, if we know the speed of sound of the WD at every radius (speed of sound is not a constant throughout the WD), we can compute the period T. As mentioned, one can use the polytrope, in Eq. (29) to evaluate a WD, and note that sound speed c_s is given by

$$c_s^2 = \frac{\partial P}{\partial \rho}. \tag{60}$$

Therefore, one can get the speed of sound expression as

$$c_s = \sqrt{\frac{\gamma P}{\rho}} = \sqrt{\gamma k \rho^{\gamma - 1}}. \tag{61}$$

So to be exact, one can compute c_s at every grid point and integrate out the total time needed for a wave to travel back and forth for an oscillation. Or if we can get an effective speed of sound $c_{s,eff}$, a speed of sound that average out the density and pressure differences so that it looks like a constant, then one can compute the period T from

$$T \approx \frac{2R}{c_{s,eff}}. \tag{62}$$

These should help to verify whether or not the above FFT is correct. One can try to have a taste of it using the data at the central density of the above WD.

Table 1. Central density trial to approximate $c_{s,eff}$ of a NMWD.

ρ_c (g cm^{-3})	f (Hz) from FFT	T (s) from FFT	R (km)	P_c (barye)	c_s (km s^{-1})	$2R/c_s$ (s)	$T/(2R/c_s)$
10^{10}	0.6	1.6667	1297.993	1.0590×10^{28}	13287	0.19537	8.5308

So the above trial shows that simply using the central density can already give us a really crude verification that the WD is possibly oscillating reasonably, at least to around the same order of magnitude. surely, the factor 8.5308 is not a small deviation, showing that it is not a good enough approximation to simply use the central density. This can be understood as we take a look at the density profile of the WD.

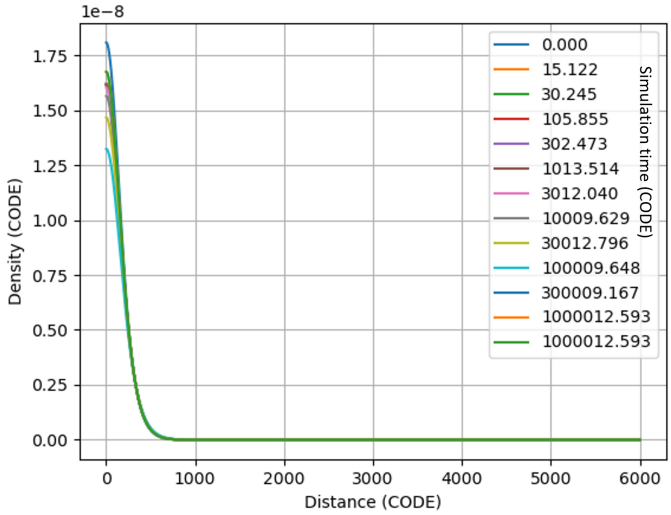

Figure 6. Density profile of the studied NMWD. The density changes quite rapidly at different radius and so it is hard to say that a certain density can be used for the computation of effective speed of sound $c_{s,eff}$, surely the central density is not the best choice. Lines in different colours show the density profile at different time step, and the legend is showing the corresponding line colour for different simulation time.

The density are concentrated at a small radius is simply a programming concern to prevent the WD from oscillating to somewhere the code cannot simulate, so we are having a large box size. But taking a look at the density profile, one can see that even for the central part of the WD is not having a relatively constant density, so taking the central density to compute $c_{s,eff}$ will be a rough approximation. Moreover, the tail of the WD is quite long, with a relatively small density so we are expecting the speed of sound there to be much smaller. As a result, if one can really consider integrating all the speed of sound and averaging them out to find the effective speed of sound, it is very possible that we can recompute the T we got from FFT.

In fact, due to our limited time in the project, we did not dig deep into the speed of sound $c_{s,eff}$ and we have only studied briefly for the frequencies from FFT for the DAWDs afterwards.

In short, the oscillation period of the left graph in Figure 4 is in a reasonable order of magnitude. Therefore, we believe the star is oscillating as expected.

3.3.1. *WENO: Normal Matter White Dwarfs Sedov Test*

As aforementioned, we had only carried out Sedov tests on NMWDs. It is basically trying to make a WD explode and the mass curve evolution typically will be like the one shown in Figure 7.

In Figure 7, x-axis spans for around 4200 s in total (i.e. around 70 minutes). As we can see, the total mass of the NMWD drops continuously from its initial mass of around 1.44 $M_{\odot}$. Therefore, it is very possibly that, given a long enough time period, the WD will no longer exist. Note that the above simulation shows the effect dynamics of more than an hour and it is very possibly that some numerical errors build up already, so it is not promising to simulate further more.

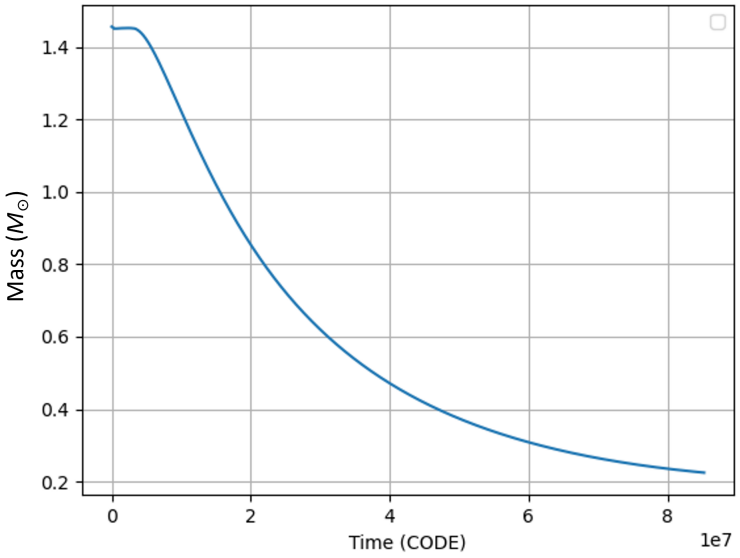

Figure 7. Total mass evolution with time under a Sedov test for a NMWD. The graph shows the time evolution for around 70 minutes in total. The total mass decreases and will eventually reaches a very small amount 0 if given enough time.

In short, the above process shows that WENO is capable to simulate a SN and it can be used for further dynamical analyses. However, this is not the main goal here and thus we did not discuss anymore on it for DAWDs.

3.4. *Fermionic Dark Matter Admixed White Dwarfs*

After computing the M-R relation for NMWDs in both gravities, we can now see what the effect of admixing FDM is. Firstly, assuming they are in hydrostatic balance, we can produce some FDAWDs. In fact, the results are now more complicated as we have DM particle mass m_d as a parameter too.

To see if our work is really producing promising results, we had tried to reproduce the graphs from others. In Figure 8, we tried to plot the NM central density $\rho_{c,n}$ against the total DM enclosed mass M_d, after constraining the total mass $M_t = 0.6\ M_\odot$ and DM particle mass $m_d = 10$ GeV.

And this is what we had reproduced as the plot from a paper researching DAWD Leung et al. (2013), showing that our results are promising. Besides, this plot also worths to be looked into. It shows that for the central density of NM to increase, the total DM mass increases, but getting faster and faster. This is an universal property, not only for the case of $M_d = 0.6\ M_\odot$ and $m_d = 10$ GeV.

One may wonder, seems like we can then get any total DM mass as we want following the curve. It is not the case actually, as the WDs we observed are only around 1 $M_\odot$, extreme cases like super-Chandrasekhar WDs are around $2M_\odot$, we cannot get a lot more FDM admixed for $m_d = 10$ GeV.

Here, one parameter is quite useful and should be introduced, the mass ratio of DM total mass to the total enclosed mass, denoted as ε, given by

$$\varepsilon = \frac{M_d}{M_t}. \tag{63}$$

This mass ratio is more useful as for the observation, we can only extract the total mass data, but not for each component. So if any model with a predicted mass ratio admixed is correct, we can directly know what fraction of the total mass is from DM.

In fact, for a WD with M_t around 1 $M_\odot$, we can seldom see M_d from FDM to be large, equivalently, we usually see ε for FDAWDs to be small. This is also discussed in a paper regarding HWDs, showing that if ε is large for a

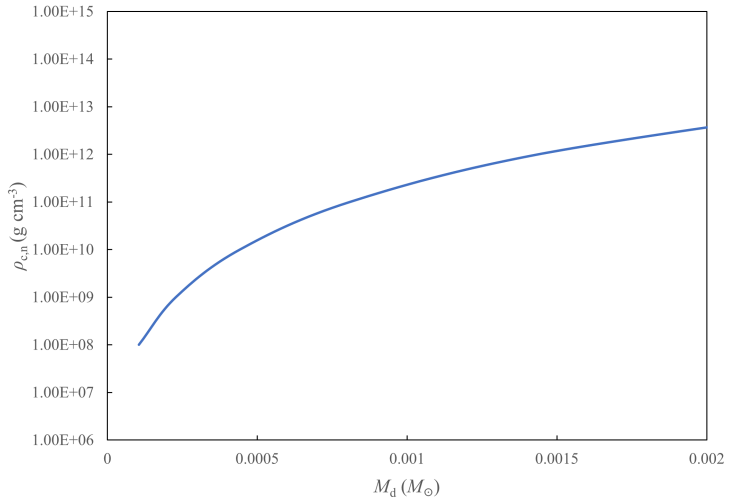

Figure 8. NM central density $\rho_{c,n}$ against total DM mass M_d under the constraint $M_t = 0.6\ M_\odot$ and $m_d = 10$ GeV. It shows that for a higher NM central density, we can admix a lot more DM into the WD.

typical WD with $M_t \approx 1\ M_\odot$ and using massive FDM particles, one would require a NM central density too high to be stable, reaching the nuclear-matter density Leung et al. (2013). Therefore, for massive FDM, the allowed ε is quite small and actually for $m_d = 1$ GeV, the maximum allowed M_d admixed $\approx 0.1\ M_\odot$ Leung et al. (2013).

Note that the total mass of DM and the DM profile depends on the DM particle mass m_d, so the above arguments are mainly for WIMP instead of axion-like particles (ALP), which are much lighter.

3.5. *WENO: Fermionic Dark Matter Admixed White Dwarfs*

After knowing that FDAWDs usually contain not much FDM using WIMP, we take a look at the properties of FDAWDs. Here we thought that for different relative structures of NM to DM in FDAWDs may result in totally different properties, therefore we divide FDAWDs to three main cases to study. Case 1 refers to NM radius R_n is largely greater than DM radius R_d (i.e. $R_n \gg R_d$), referring to a DM core. Case 2 refers to the two fluids are having similar radii (i.e. $R_n \approx R_d$). Case 3 is that NM radius is much smaller than DM radius (i.e. $R_n \ll R_d$), which is a WD in a DM halo.

Before going deep into each cases, as aforementioned, the DM total mass and the profile, therefore radius, depends on m_d a lot. In fact, $R \propto k$, which is the k in Eq. (29) and k relates to the pressure. So for NM, electrons are the one providing the degeneracy pressure and thus $R_n \propto k_n \propto m_e^{-1}$; while for FDM, they themselves provide the degeneracy pressure and thus $R_d \propto k_d \propto m_d^{-8/3}$. Then when using the same m_d one can usually get a profile with similar radi, not varying much. So when studying the cases, the main parameters governing the cases is m_d. And generally Case 1 with a DM core is usually the results of a heavier DM particle comparing to Case 3 with a DM halo.

3.5.1. *Case 1: FDAWD with a Dark Core*

After conducting several combinations of simulations for Case 1, generally there are typical properties for FDAWDs with a dark core.

Note that we are also implementing some initial velocities to the WDs, for NM in the cases below, but they wont affect the main properties to be discussed. Surely that different velocity profiles are affecting the motion of the star, and they will be discussed later in this section.

For a FDAWD with $\rho_{c,n} = 10^{10}$ g cm^{-3} and $\rho_{c,d} = 10^{11}$ g cm^{-3}, here we use $m_d = 1$ GeV, and we have set the initial velocity profile for DM component to be 0 everywhere, then we can see the oscillation of both central density to be neraly SHMs.

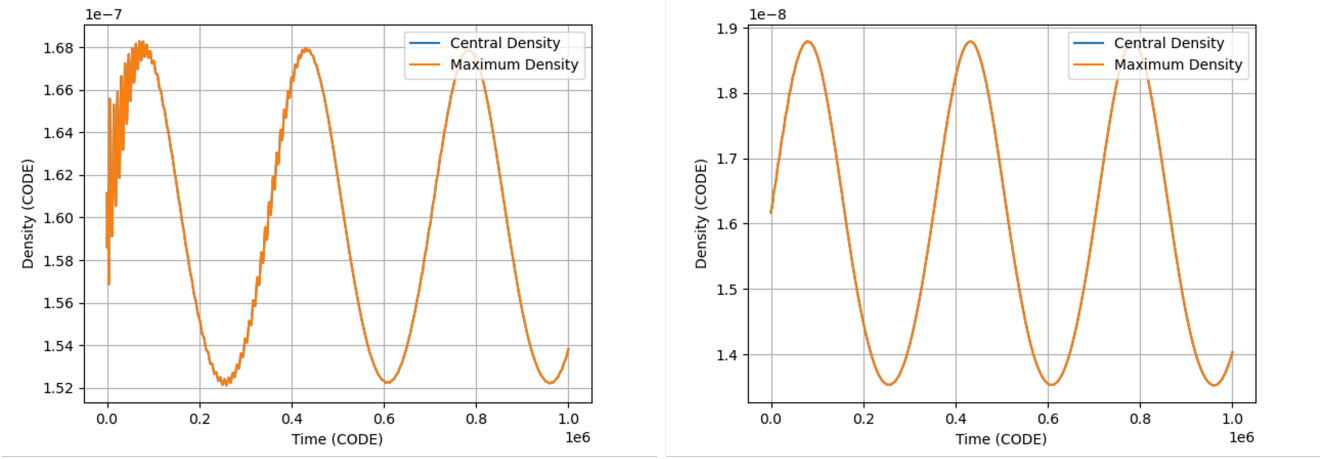

Figure 9. (Left) Time evolution of the central density of DM $\rho_{c,d}$ for a FDAWD with a dark core. There exists two major oscillations, a low frequency SHM and a high frequency oscillation, which damps and may be the oscillation due to its small radius. (Right) Time evolution of Central density of NM $\rho_{c,n}$ for a FDAWD with a dark core. There is a SHM.

In fact, what is general here is that it seems that for NM, it is still undergoing SHM, not really affected by the fact that there is a DM core. This is anticipated as we are having $R_n \gg R_d$, making that in the NM point of view, it seems to have just a slightly more amount of mass in the centre, or a point source mass in the centre. This should not affect its fundamental oscillation pattern and period by a lot. And this can be verified by using FFT again. The FFT graphs for this case is nearly the same as Figure 5.

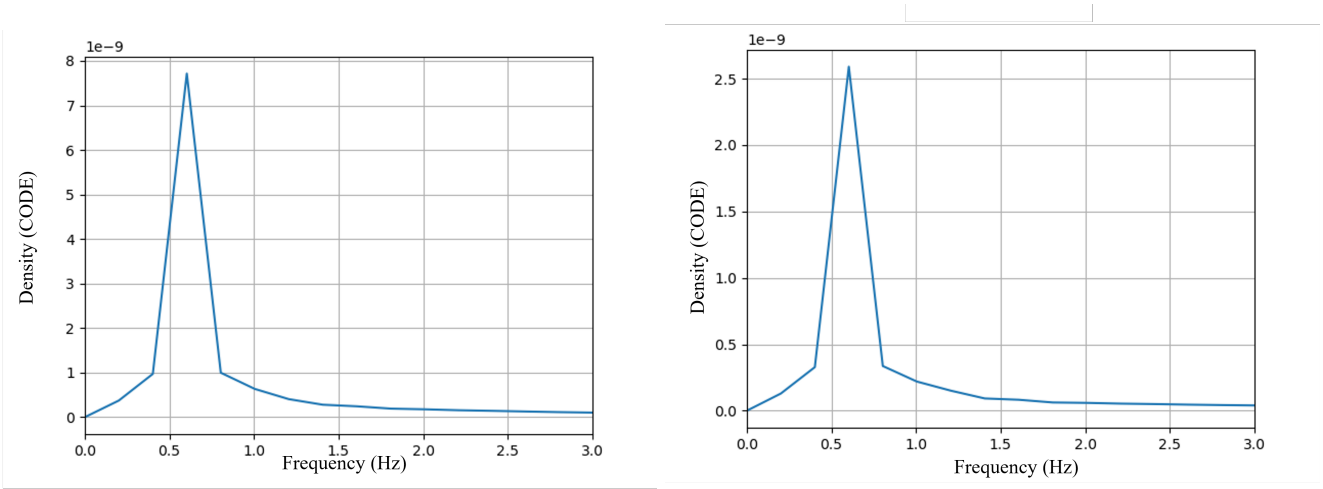

Figure 10. (Left) FFT plot of DM central density for a FDAWD with a dark core. (Right) FFT plot of NM central density for a FDAWD with a dark core. They are basically the same, without a higher peak for the left panel may possibly due to the range of FFT resolved is not high enough. These two graphs show that they are oscillating in the same frequency, DM is affected by NM and follows its motion.

Here we can see that the right panel of Figure 10 is nearly the same as Figure 5, it proved that by adding a DM core to a WD with no initial velocity, we cannot see much changes in oscillations, as expected. From the DM central

density plot, we can also see that DM core is having an oscillation with higher frequency and it damps with time goes on, showing that this is not another normal mode and the system is suppressing this oscillation, getting to oscillate in their normal modes only, and the WD is therefore stable. Verified in Figure 10, they are having the peaks at the same frequency, showing a normal mode. We cannot see a higher frequency peak in the FFT is simply because the plot does not contain that frequency range.

While comparing the two graphs in Figure 9, we can see the two fluids oscillate at the same phase at all the time, despite the higher frequency oscillation for DM. The high frequency basically arises from the small radius of DM component so it has nothing to do with any fancy physics.

In order to study whether we are able to produce an out-of-phase oscillation, which should be another normal mode of the system, the same setting has been used with modification: a FDAWD with $\rho_{c,n} = 10^{10}$ g cm^{-3} and $\rho_{c,d} = 10^{11}$ g cm^{-3}, here we use $m_d = 1$ GeV, but we are now setting the initial velocity profile of DM to be in the opposite direction of that of NM. Something crazier is then seen, but the main properties remain.

Here we plot again the central densities time evolution for a FDAWD with an opposite direction initial velocity profile for the two fluids in Figure 11.

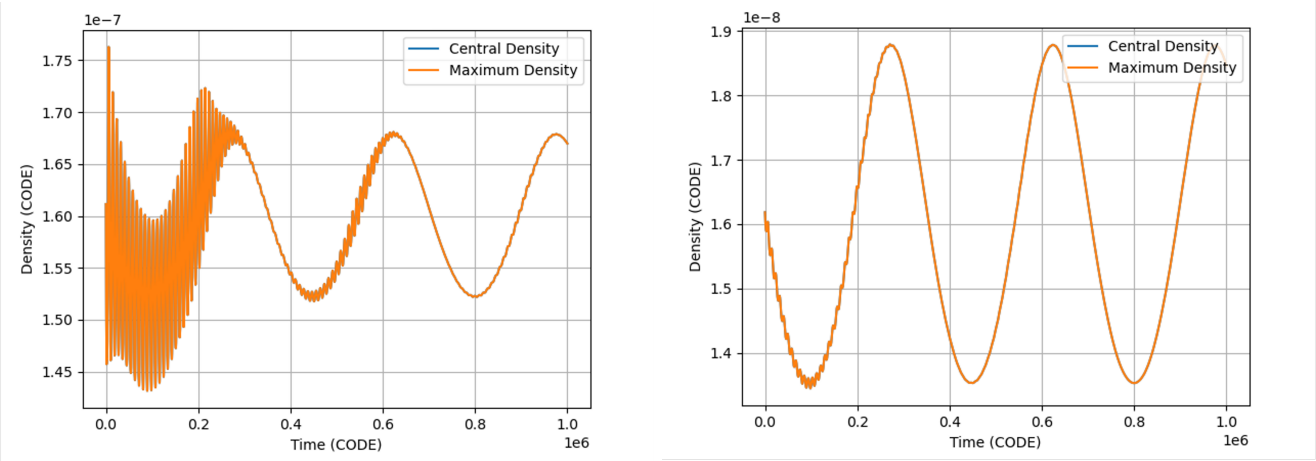

Figure 11. (Left) Time evolution of central density of DM $\rho_{c,d}$ for a FDAWD with a dark core. Again a damping in the high frequency oscillation damps and it follows the motion of NM. (Right) Time evolution of central density of NM $\rho_{c,n}$ for a FDAWD with a dark core. SHM is the main part of the graph, but with some higher frequency oscillation, induced from DM, can be seen at the very beginning. This vibration is damped.

So similar observations can be made, they are vibrating in phase for the fundamental normal modes, because that is the NM normal modes and this dominates the motion of DM through gravity as $M_n \gg M_d$. Moreover, we can see that as the motion of DM is damping so as to reach a lower energy state.

More than that, with the small radius of DM, the implementation of opposite velocity profile does not affect the motion of the phase by much as the frequencies are not comparable.

And something more to be seen here is that, for NM, they are now affected by the initial motion of DM, seen as some higher frequency oscillations, that is unobservable in Figure 9, probably because all the oscillations are initiated by NM there.

Usually, the out-of-phase oscillation is also a normal mode for a two-fluid system, but we are not able to trigger it yet, probably because of its high excitation energy. And this depends on whether the two fluids' polytropic k are comparable, as the speed of sound c_s depends on it, surely also depending on density, by Eq. (61). Therefore, for

Case 1, the k differs by a lot for the two fluids and so as their density at each radius, this is hard to be seen.

In short, for a FDAWD with a dark core, we should expect the NM to oscillate in its own frequency, just as a NMWD does, not affected much by the DM core oscillation as it is damped. The two fluids oscillate in phase.

3.5.2. *Case 2: FDAWD with similar radii for the two fluids*

Before discussing the results, one should note that it is really hard to find a combination of parameters to yield a DM component to be of comparable size with NM, as the phase transition between DM core and DM halo is fast. Therefore, the following discussion is based on the only case we had successfully made, and it is possible that the properties mention here may not be universal for Case 2, but probably still provide some insights.

Here we have used a WD with approximately the same radius, and the parameters are $\rho_{c,d} = 6.7 \times 10^8$ g cm^{-3}, $\rho_{c,n} = 10^{10}$ g cm^{-3} and $m_d = 0.1$ GeV. Trying to study the out-of-phase oscillation, we have used opposite initial velocity profiles here too.

Table 2. Results of a FDAWD with similar radii for the two fluids.

M_d ($M_\odot$)	M_n ($M_\odot$)	R_d (km)	R_n (km)	M_t ($M_\odot$)	R_n ($R_\odot$)	ε
0.22606	1.2261	1207.18	1185.03	1.4522	0.0017034	0.15567

For the masses and radii of both NM and DM of this Case 2 WD, they are shown in Table 2. Actually, here in this case we get a WD near the Chandrasekhar limit, so more FDMs are admixed, and we are using lighter m_d, compared to the statement that we shall find not much FDM in a FDAWD for a usual WD with massive DM particle.

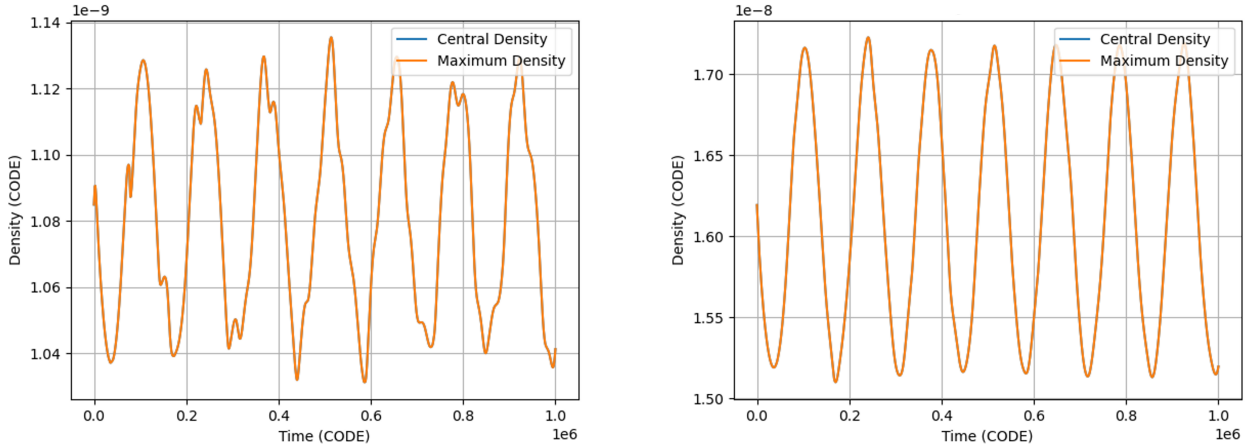

Figure 12. (Left) Time evolution of central density of DM $\rho_{c,d}$ for a FDAWD with similar radii for the two fluids. There are some weird patterns, showing an admixture of oscillation of some other frequencies. (Right) Time evolution of central density of NM $\rho_{c,n}$ for a FDAWD with similar radii for the two fluids. The SHM shown here is unanticipated.

Taking a look at the time evolution graph of the central densities of the fluids in Figure 12, they are pretty interesting. For the right panel showing the time evolution of NM cnetral density, it is again undergoing a SHM, seems not to be affected by the DM component.

While for DM, there is an oscillation of different frequencies. This is not expected, but at least they are also under the same fundamental frequency, probably a normal mode of the system. What we expect here is that the NM is

affected by the DM and exhibits an oscillation as a wave packet. This is not the case here, probably because the total mass of DM is not large enough comparing to M_n.

Another important point to study is that, even with an initial set of opposite velocity profiles, and we did see that at the very beginning of the oscillation, the DM try to vibrate out-of-phase, but it follows the NM again shortly after the start of simulation. This reviews that the out-of-phase oscillation is probably really hard to excite.

3.5.3. *Case 3: FDAWD with a Dark Matter Halo*

For a FDAWD with a DM halo, we can see different sorts of properties. Note that in this case, M_d is large, as we required R_d to be large. But for observation, what we are seeing is only NM and probably will not be able to include the mass at a radius a lot larger than R_n. Therefore, in fact, these properties is meaningful to a WD with reasonable M_n in a DM halo instead of considering the whole halo size.

If one would like to study the FDAWD with a DM halo with $R_d \gg R_n$, one can also reduce m_d as mentioned $R_d \propto m_d^{-8/3}$ but this is not studied here.

Here, the used WD is formed from $\rho_{c,d} = 10^{10}$ g cm^{-3}, $\rho_{c,n} = 10^{10}$ g cm^{-3} and $m_d = 1$ GeV with opposite direction initial velocity profiles.

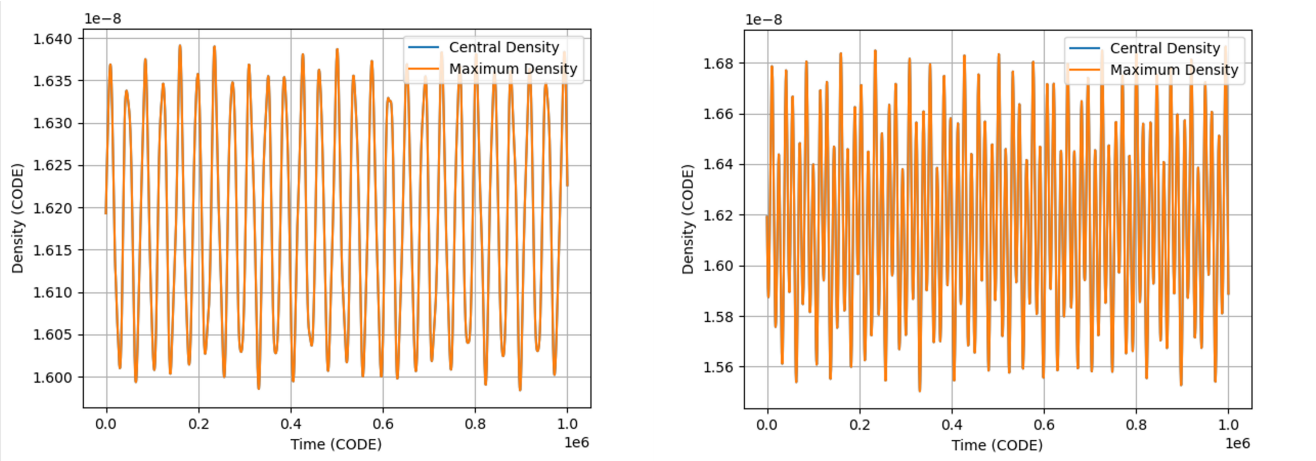

Figure 13. (Left) Time evolution of central density of DM $\rho_{c,d}$ for a FDAWD with a DM halo. It is not affected by the NM much and exhibits a SHM, just like NM does in previous cases. This is probably the fundamental mode of DM. (Right) Time evolution of central density of NM $\rho_{c,n}$ for a FDAWD with DM halo. Complicated pattern can be seen, showing it is affected by the DM, and trying to follow its motion too. But there is still some NM initiated motion that can sustain.

As mentioned, M_d is large, and the oscillation of DM is basically unaffected by NM. It is similar to Case 1, but reversed in the two fluids. The NM fluid exhibits another higher frequency oscillation, arises from the small radius of it. The high frequency oscillation is not seen to be damped yet, and so it may be a higher resonance too, adjusted from the NM own oscillation. And it follows the oscillation of DM too, instead of having an out-of-phase vibration.

In short, we can conclude that whenever one fluid is spanning a lot further than the other, or one fluid is being a lot more massive than the other, we will find the fluid to be undergoing SHM in its own normal mode. Then the other one will follow this SHM and oscillate, probably with some higher frequencies too. And it is expected to find the fluids vibrate in phase, rarely out-of-phase.

3.6. *Bosonic Dark Matter Admixed White Dwarfs*

To study BDAWDs, remember that as mentioned, $\frac{a_s}{m_d^3}$ is a single parameter, and it is the most essential part of BDAWDs. Therefore we can first use a fixed setting of NM and DM central density and then vary the above parameter, to see how does it affect the WD and its ε. We first assume that a_s is a constant (always the same interacting strength) throughout the star.

Using the TOV corrected BDAWD governing equations, most generally, we can see that ε varies with dimensionless $\frac{a_s}{m_d^3}$ (i.e. $\frac{a_s m_p^3}{a_0 m_d^3}$, where a_0 is the Bohr radius) as a S-shaped curve, which is probably a logistic curve. In Figure 14, we show that the relation for a BDAWD with $\rho_{c,d} = 10^{11}$ g cm^{-3}, $\rho_{c,n} = 10^{1}0$ g cm^{-3}, $m_d = 1$ GeV with the changing a_s.

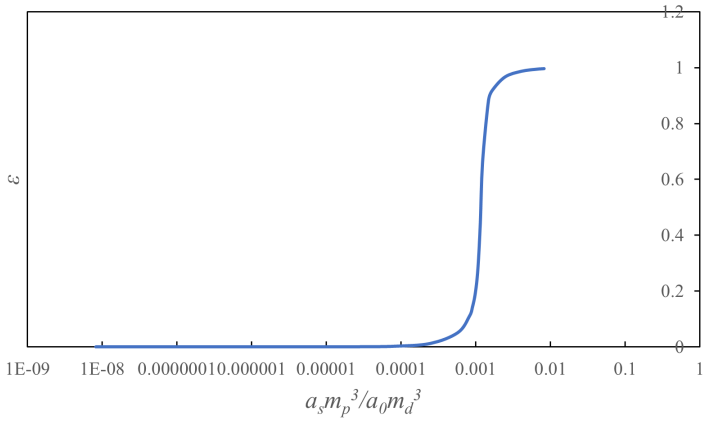

Figure 14. General shape of mass ratio ε against $\frac{a_s m_p^3}{a_0 m_d^3}$. It is universal that we will find a sigmoid curve for other WDs. This is possibly be a logistic curve. Note that the phase transition of a BDAWD from NM-dominated one to DM-dominated one is fast.

The above graph involves two major parts, with NM highly-dominated one, which means a small (< 0.1) ε; and a part with DM admixing becomes important ($\varepsilon \leq 0.1$). For the NM highly-dominated part, one can actually find a exponential relationship.

Plotted in Figure 15, one can see that there are consistent slopes for all the lines, those curves are basically the same curve in Figure 14 but only in the log-log graph.

Table 3. Constants for ε vs $\frac{a_s m_p^3}{a_0 m_d^3}$ relation in the form of $\varepsilon = A\left(\frac{a_s m_p^3}{a_0 m_d^3}\right)^{\alpha}$.

$\rho_{c,d}$ (g cm^{-3})	$\rho_{c,n}$ (g cm^{-3})	Prefactor A	Index α
10^{11}	10^{10}	2852.6	1.4917
10^{10}	10^{10}	116.9	1.5124
3×10^{9}	3×10^{9}	36.515	1.5144
3×10^{8}	10^{7}	21.288	1.5093
3×10^{8}	3×10^{9}	0.2189	1.5135

From Table 3, we can probably conclude that the index α should be having the value 3/2 regardless of the central densities of the two fluids. While it is hard to tell the relationship between the prefactor A and the central densities.

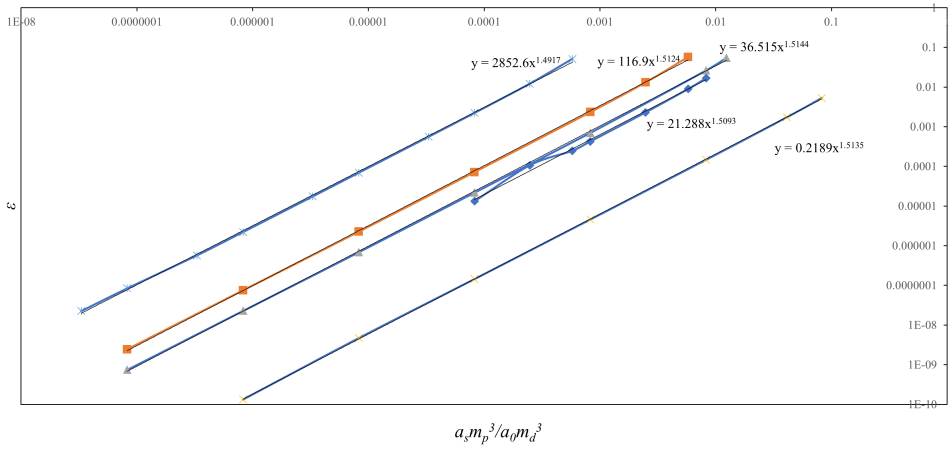

Figure 15. Log-log graph of ε against $\frac{a_s m_p^3}{a_0 m_d^3}$ for NM highly-dominated part. Different curves refer to different set of parameters $\rho_{c,d}$ and $\rho_{c,n}$ are used. The same slopes of different straight lines show that this exponential relationship is universal and this is the result of some property of the NM in a WD.

Due to the limited time for the project, the quantitative explanation of why $\alpha = 3/2$ is not studied. But as they are NM-dominated WDs, this universal slope should be a constant arises from the EOS for a NMWD.

However, what is really important is that there are noticeable amount of DM being admixed, so the above relation may not be stunning at all. Therefore we pay more attention to study the part where DM admixing is important.

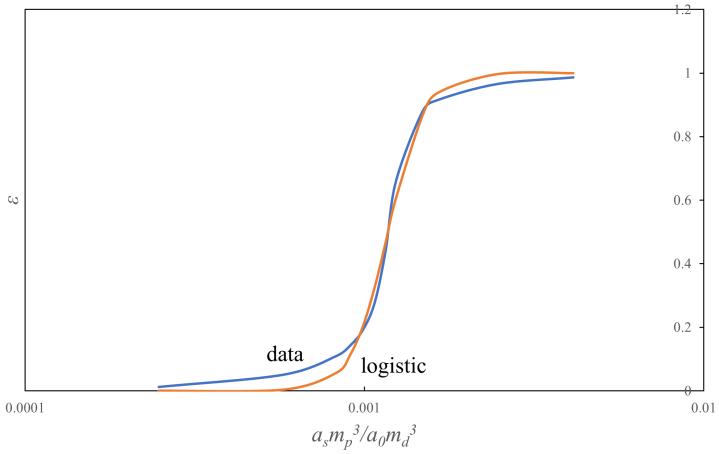

Figure 16. Logistic curve fitting for mass ratio ε against $\frac{a_s m_p^3}{a_0 m_d^3}$ for noticeable DM admixing. The blue curve is the data we got from the code; and the orange curve is the fitting of the logistic curve. The parameters used to fit the curve do not provide any clue on their analytical forms.

Note that for any set of setting parameters $\rho_{c,d}$, $\rho_{c,n}$ and m_d, we will surely have different x-axis ranges, but the shape is still the same and they can also be approximated by a logistic curve. However, we cannot get an analytical relationship between the parameters defining a logistic curve and the above setting parameters. From the graph, we can also see that the curve shows a quick phase change between a NM-dominated BDAWD and a DM-dominated BDAWD. To find them to be at equal masses will be a bit difficult.

One very important point to see is that, the above curve never includes a negative scattering length $a_s < 0$. This is because whenever a_s is negative, which is an attractive interaction, then the celestial body formed is no more a WD but turns into a BH. This is also true even for only a part of the star is having negative a_s.

Then if we plot the M-R relation for a BDAWD of same setting parameters with different a_s/m_d^3, we can find it to be a C-shaped curve, shown in Figure 17.

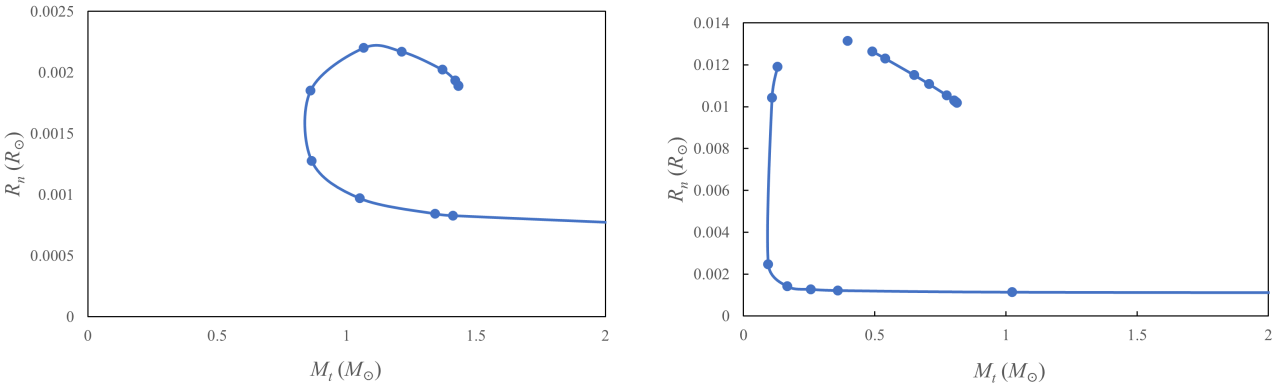

Figure 17. (Left) The general M-R relation is C-shaped when one consider a BDAWD with the same setting parameters but different a_s/m_d^3. (Right) The case of the C-shaped curve splits, at around $R_n \approx 0.013\ R_\odot$.

This shows that, firstly we can actually get a very massive BDAWD, which is DM-dominated with a small radius. Note that we have check that it is not a BH, so it is simply a WD in a massive BDM halo, up to any mass we want. Besides, we are then able to see that we can get some super-Chandrasekhar WDs and some small M_t large R_n WDs. BDAWD can then be used to explain the existence of those WDs.

More specially, there seems to be a cap where R_n of the WD cannot exceed somewhere around $0.013\ R_\odot$. This is something that is unexpected but seen in cases that the R_n are large (for BDAWD). It may therefore be an upper-bound of R_n for a BDAWD and requires further explanation.

Note that whether the curve looks like a 'C', or little bit distorted or even splitting up in the right panel of Figure 17, they depends on the ratio between the two central densities. For $\rho_{c,d}$ to be smaller than $\rho_{c,n}$, we will get a curve with the C-part to be really small; for they are the same, we will get a nice C-shape just as the left panel in Figure 17. And for $\rho_{c,d} > \rho_{c,n}$, we can have a curve enabling small M_t, small R_n BDAWDs and also some small M_t but large R_n BDAWDs just as shown, or even with splitted curves.

Plotted in Figure 18, we show the distribution of possible BDAWDs in the M-R relation plot, together with the plot of NMWD M-R relation, to have a better understanding.

From the plot, we can easily see that basically all WDs with $R_n \leq 0.013\ R_\odot$ and simultaneouly under $NMWD$ allowed curves are possible, if we have enough data points and plot them out. Moreover, super-Chandrasekhar WDs with small radius is also possible, to any amount of total mass. This is really stunning to get a range of possible WDs and they can be used to explain some interesting WDs.

3.7. *WENO: Bosonic Dark Matter Admixed White Dwarfs*

After getting possible ranges of BDAWDs by assuming they are in hydrostatic balance, one important thing is to check whether they are stable so that they can really exist and be detected. To do this, we have to use WENO and

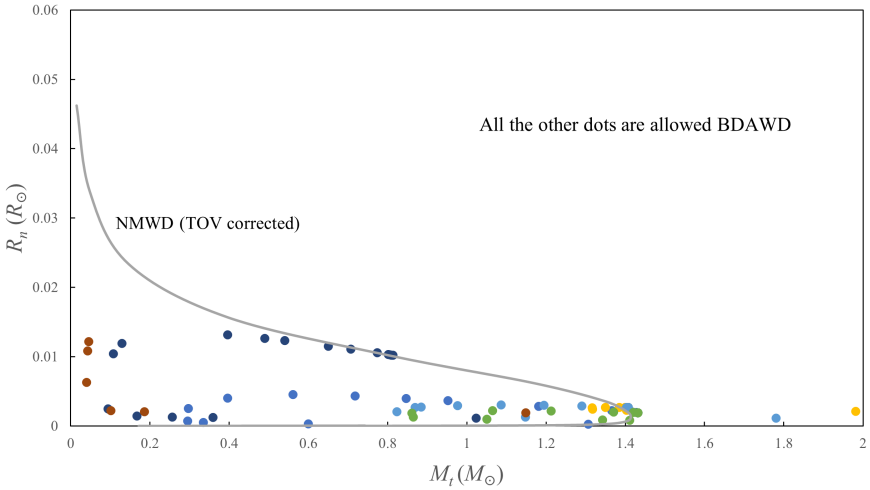

Figure 18. M-R distribution for BDAWDs vs relation for NMWDs (TOV corrected). Different colours are data points generated from different sets of $\rho_{c,d}$, $\rho_{c,d}$; and the data points with the same colour refer to WDs with different a_s/m_d^3 for the same central densities. The grey line is the M-R relation for NMWDs (TOV corrected). A cap of $R_n < 0.013\ R_\odot$ can be seen and the area under both $0.013\ R_\odot$ and the NMWD M-R relation, together with the super-Chandrasekhar WDs are allowed with BDM admixed.

use hydrodynamical equations to see their evolutions.

In the upcoming discussion on hydrodynamics of BDAWDs, we had picked two special cases: one is a super-Chandrasekhar WD, another one is a small M_t large R_n WD. Both are the WDs that may not be stable at first glance and requires further investigation. Moreover, it is likely that for a star which is unstable, the oscillation can cause it to collapse further or the matter are not tightly bounded. So these two cases may serve as the upper and lower bounds of stability for BDAWDs. The others are therefore assumed to be stable.

Before studying the evolutions of BDAWDs, the quantum potential term $\frac{1}{m_d}\nabla Q$ should first be examined for its importance, if not, one can drop it. In fact, the data points at each grid are used for computing the value for each force term in Eq. (48), then one can get the importance of the quantum potential term by finding the ratio of this term to the others.

For the two cases aforementioned, one can find the maximum Q-importance ratio in Table 4.

Table 4. Maximum Q-importance ratio for the two cases of BDAWDs.

$\rho_{c,d}$ (g cm^{-3})	$\rho_{c,n}$ (g cm^{-3})	m_d (GeV)	a_s (a_0)	Maximum Q-importance ratio
3×10^8	10^7	1	0.029	$\mathcal{O}(10^{-32})$
10^{10}	10^{10}	1	0.04	$\mathcal{O}(10^{-36})$

In view of the very small maximum Q-importance ratios shown in Table 4, one can believe that the term will basically have no effects on the star and thus it is ignored for all BDAWD computations.

Then one can use the WENO code to see the hydrodynamical effects. One can also suspect that the TOV corrections may also affect the stars' evolution. It is surely true but it only affects the stars' total masses and radii within a range of 5 %, usually within 2 %. So the upcoming data can still be regarded promising.

3.7.1. *Super-Chandrasekhar Bosonic Dark Matter Admixed White Dwarfs*

We first investigated the hydrodynamics of the super-Chandrasekhar BDAWD. The WD we used is governed by $\rho_{c,d} = 10^{10}$ g cm^{-3}, $\rho_{c,n} = 10^{10}$ g cm^{-3}, $m_d = 1$ GeV and $a_s = 0.04\ a_0$. Then the results are shown in Table 5.

Table 5. Results of a super-Chandrasekhar BDAWD with $\rho_{c,d} = 10^{10}$ g cm^{-3}, $\rho_{c,n} = 10^{10}$ g cm^{-3}, $m_d = 1$ GeV and $a_s = 0.04\ a_0$.

$M_d\ (M_\odot)$	$M_n\ (M_\odot)$	R_d (km)	R_n (km)	$M_t\ (M_\odot)$	$R_n\ (R_\odot)$	ε
1.8435	0.29925	700.24	529.53	2.1427	0.00076115	0.86034

So for this case, we can see how the central densities of both fluids oscillate.

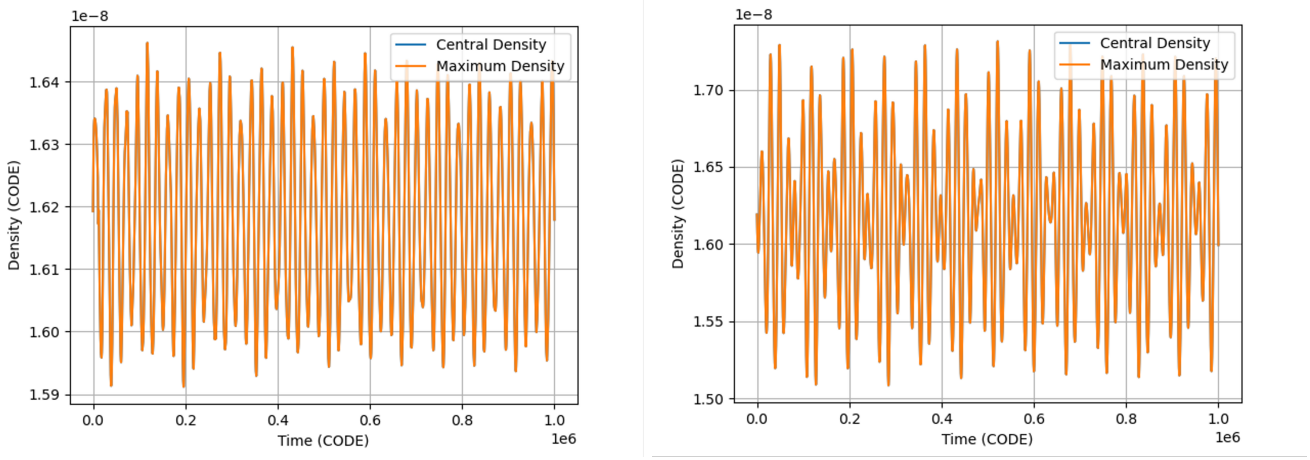

Figure 19. (Left) Time evolution of central density of DM $\rho_{c,d}$ for a super-Chandrasekhar WD. The plot is full of high frequency oscillations. (Right) Time evolution of central density of NM $\rho_{c,n}$ for a super-Chandrasekhar WD. An envelope of wave can be seen.

The plots of both central densities against time are shown in Figure 19. The most important thing is that, these two plots show that the super-Chandrasekhar BDAWD is stable, so BDM admixing in a WD is a possible explanation of the existence of those super-Chandrasekhar limit.

Besides, some interesting properties can also be seen here. Especially in the right panel, one can easily see there are two frequencies of oscillation and there is an wave envelope. This is not really seen before, as obvious as this, because this show that there are two oscillations of a frequency that is similar.

And in fact when one compares the FFTs of the two central densities evolutions, shown in Figure 20, one can see that there are two main peaks at the same frequencies in both graphs. And they are quite close to each other, showing how the envelop of wave arises. They are probably the normal modes of the system, or else the oscillation may by suppressed quickly.

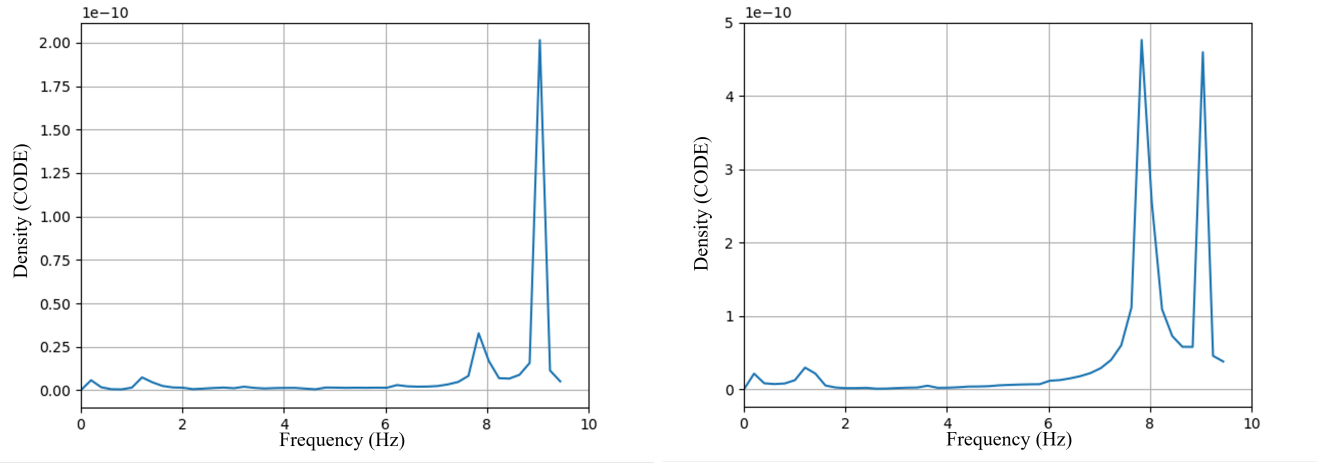

Figure 20. (Left) FFT plot of DM central density for a super-Chandrasekhear WD by BDAWD. (Right) FFT plot of NM central density for a super-Chandrasekhar WD by BDAWD. They are having peaks at the two same frequencies, and answered the formation of the wave envelope.

The similar frequencies may be a result of the similar radii for the two fluids. But all in all, it is possible to form a wave packet in oscillation, which is not seen even for the similar radius case for FDAWD in 3.5.2.

3.7.2. *Small M_t large R_n Bosonic Dark Matter Admixed White Dwarfs*

Again we would most importantly try to see whether the WDs are stable. We have used opposite initial velocity profiles too to see if out-of-phase oscillation can be seen here.

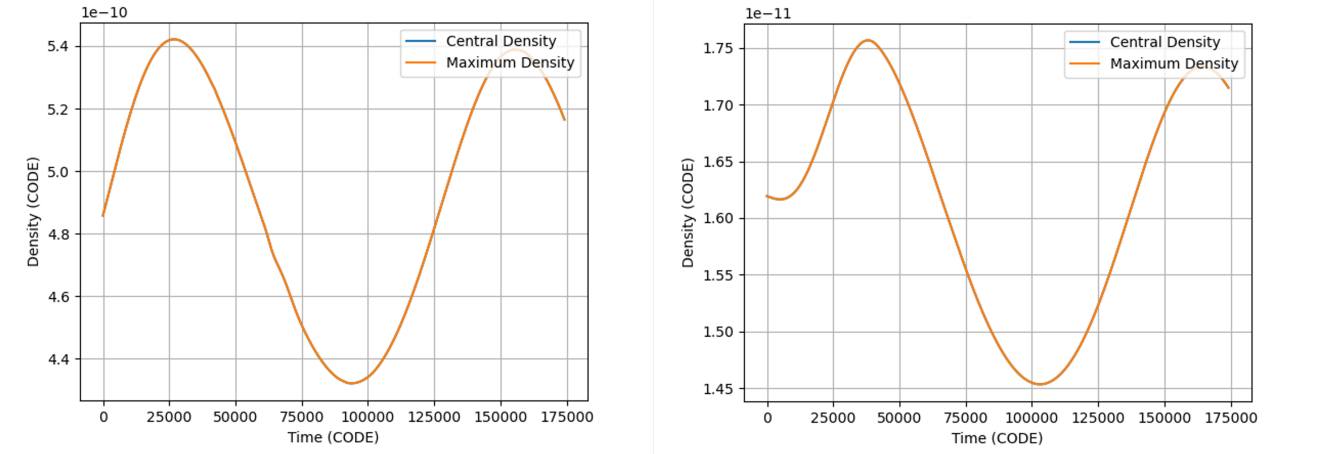

Figure 21. (Left) Time evolution of central density of DM $\rho_{c,d}$ for a small M_t large R_n WD by BDAWD. A cycle of oscillation had just been completed, showing a large chance for it to be a stable WD. (Right) Time evolution of central density of NM $\rho_{c,n}$ for a small M_t large R_n WD by BDAWD. It shows that WD is possibly stable too. An interesting feature is that the original out-of-phase motion of NM in the very beginning had changed and NM follows the motion of DM again in shortly after the start of simulation.

From Figure 21, one can tell that they are also stable, as they are not deviating much and able to get back to their initial phases. There are only one period of oscillation is simply due to some numerical error and not much time span

is simulated, but we can still very possibly tell it as a stable WD. This explains the existence of these BDAWDs. Therefore, we should be able to observe these small M_t large R_n BDAWDs.

More than that, again we can see that one fluid follows the other's oscillation very shortly after the start of simulation, despite their initial out-of-phase vibrations. Showing that they prefer the lowest energy normal mode, vibrating in the same phase and illustrate that the out-of-phase vibration for this WD is also hard to excite. These properties are basically the same as FDAWD, showing that one may not verify whether the DM fluid is formed from FDM or BDM if only the oscillation pattern of NM is considered. Nature of DM should be determined by other results, maybe from ε.

3.8. *Variable Scattering Length* a_s

Again here we use the above two special cases from BDAWDs to take a look at the effect of variable a_s on M_t.

In Eq. (59), the governing parameter is η and therefore the graphs of M_t against η are plotted. Note that for the upcoming discussion, we use

$$\rho_{d,crit} = \rho_{c,d}/e. \tag{64}$$

This is just a way of defining a scale of ρ to be the critical density, and we have no clues which is the real critical density. Note that with the definition of Eq. (59), positive η means that BDM in the internal part of the WD is becoming less repulsive while the outer part is becoming more repulsive. Vice versa for negative η.

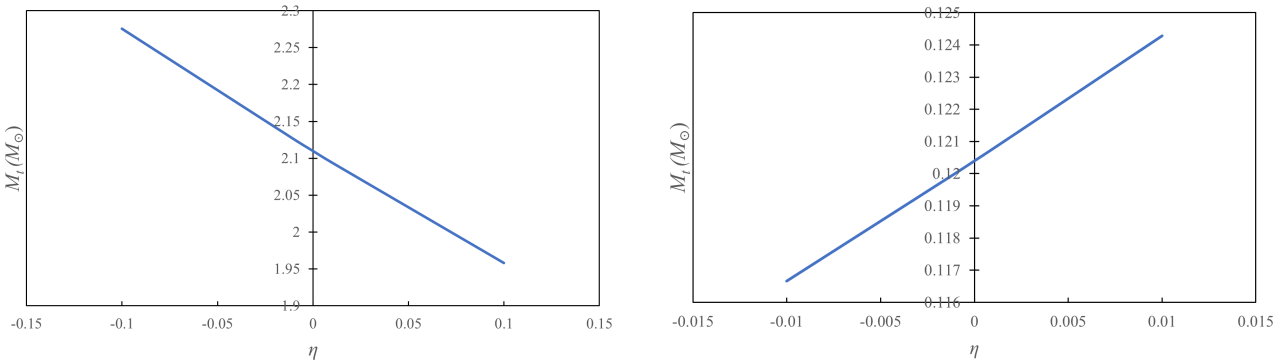

Figure 22. (Left) Total mass M_t of BDAWDs against the constant η for super-Chandrasekhar WDs. The plot shows a linear relationship, increasing η will result in decreasing total mass M_t. (Right) Total mass M_t of BDAWDs against the constant η for small M_t large R_n WDs. The plot is also a linear relationship, but with a positive relation, which is different from the graph on the left.

Figure 22 shows that when η changes, the total mass M_t may increase or decrease, linearly. This linearity is something we did not expect. It is understandable that for small η, the changes is small. But the different direction of changes worths studying.

Therefore, more M_t against η plots are made and one can find that, it is probable that this increasing or decreasing is governed by the radius ratio of two fluids R_n/R_d when the whole star is under the same a_s (i.e. $\eta = 0$).

Then, a short conclusion is that when $R_n/R_d \approx 2.4$, the proportionality of M_t of η changes, from decreasing to increasing. Actually we have no clues for the cause as we are creating some unknown physics. This worths further studies.

One point to add is that, for $\eta = 1$, the star formed is a BH. This can be explained, due to our definition of $\rho_{d,crit}$, it causes the central part to experience a negative a_s, and thus contains a BH, with no supporting pressure to balance the gravity. It is another way proving that whenever there is a negative a_s, a BH is formed.

3.8.1. *WENO: Varying a_s*

To check whether a BDAWD with different a_s possibly exists, is again relying on WENO code. As one can see there are two kinds of relationship between M_t and η, one shall check for both cases. Again we take the two special cases discussed before, the super-Chandrasekhar BDAWD and the small M_t large R_n BDAWD.

As discussed, it is expected that for small η, the star does not contain large deviation in a_s and so no much deformation shall be seen. Therefore, η is taken to be 0.1 first to see the effects.

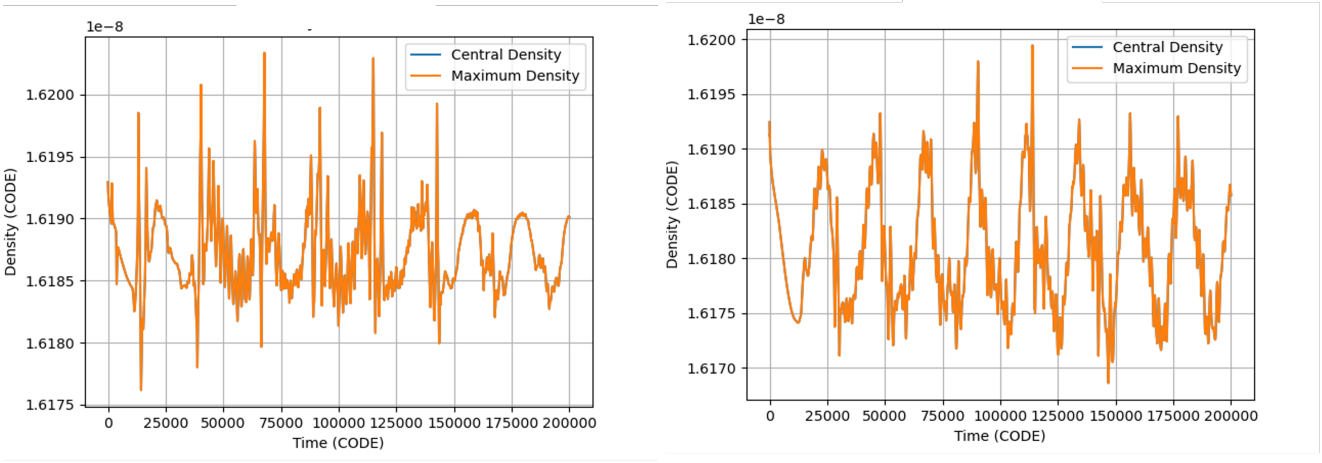

Figure 23. (Left) Time evolution of central density of DM $\rho_{c,d}$ for a super-Chandrasekhar BDAWD with variable a_s when $\eta = 0.1$. No SHM can be seen anymore and the pattern is something weird. But they can still show that they are stable and able to get back to their initial state.(Right) Time evolution of central density of NM $\rho_{c,n}$ for a super-Chandrasekhar BDAWD with variable a_s when $\eta = 0.1$. No SHM can be seen too, the smooth curve at the very beginning show that it was first undergoing SHM but then being perturbed by the motion of DM. Again, it shows that the WD is stable and thus we should be able to find it. We can also distinguish it if the oscillation pattern is not a SHM.

From Figure 23, one can surely see that they are no longer undergoing SHMs, but still they are stable, being not deviated much from the equilibrium points. It is possible that those very sharp peaks get to very large in values but they are at least being able to get back, showing a nice stability. Moreover, we can still see some couplings between the two fluids that they are vibrating with the same fundamental frequency.

Even more interesting is, for smaller η or even negative η (tested for $|\eta| = 0.1 and \eta = 0.01$) the plots are not exactly the same as Figure 23, but similar in shape and the WDs are also stable. Therefore, even for a super-Chandrasekhar BDAWD with largely varying a_s, one can still get a stable WD to be detected.

Now, for the small M_t large R_n BDAWD. The shapes of the central density time evolution curve are different.

Figure 24 shows that the deviations again are small, even for a largely varying a_s with $\eta = 0.1$ and although it seems not to oscillate by a full cycle yet, they are very possibly still stable.

And this case is also tested for $|\eta| = 0.01$ and -0.1, the shapes are again similar.

To conclude, BDAWDs with linearly varying a_s are very possibly stable and be observed, unless any part of $a_s < 0$. And this is not related to whether the total mass M_t increases or decreases with η.

4. CONCLUSION

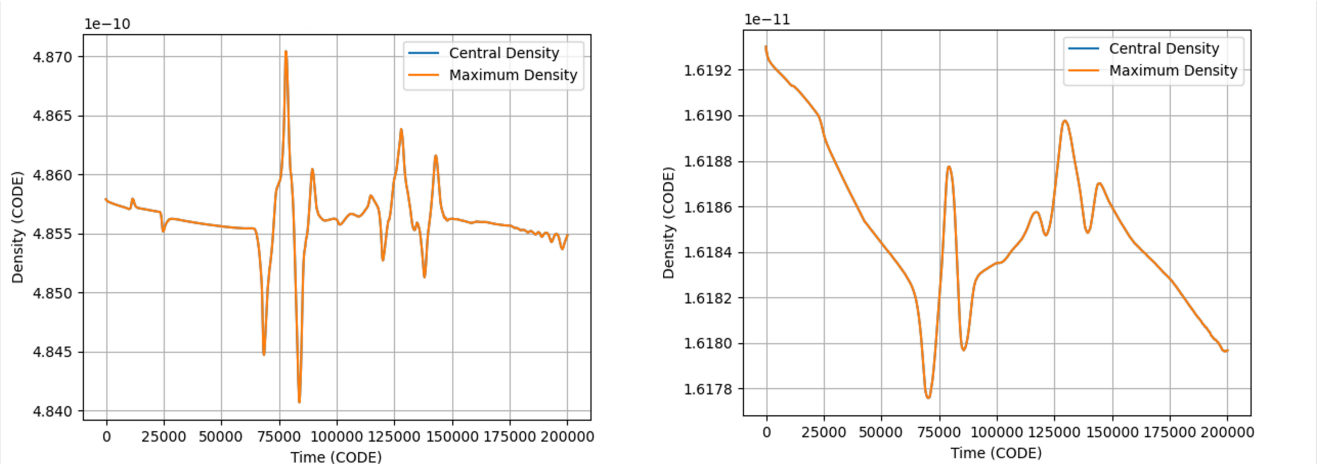

Figure 24. (Left) Time evolution of central density of DM $\rho_{c,d}$ for a small M_t large R_n BDAWD with variable a_s when $\eta = 0.1$. The pattern is another weird shape. But they can still show that they are stable and able to get back to their initial state.(Right) Time evolution of central density of NM $\rho_{c,n}$ for a small M_t large R_n BDAWD with variable a_s when $\eta = 0.1$. Only small deviations of the values are found.

BDAWDs provide another portal to explain the differences between observations and our current theory on WDs. We can produce WDs with a maximum allowed R_n to be $0.013\ R_\odot$ and no restriction on M_t. More importantly, super-Chandrasekhar WDs and small M_t large R_n WDs can be accounted using BDAWDs.

Comparing to FDAWDs, one essential property is that for WDs with reasonable total mass, BDAWDs provide the probability that larger portion of mass is from DM, with the same m_d.

Besides, it is hard to see, for both kinds of DM, that the two fluids are vibrating out-of-phase. The oscillation patterns depend highly on the relative radius and total mass of each component.

Inside a BDAWD, scattering length a_s is not necessarily a constant and it is studied if there is a linear variation of a_s depending on the DM density. Results show that BDAWDs are still stable with largely varying a_s, unless a part of the WD is experiencing negative a_s and forms a BH.

This probes the probability that to produce a BN in further study, one should require at least a part of the star to experience attractive interaction to see more dynamical evolutions and the physics beyond.

We express our wholehearted gratitude towards our supervisor, Prof. M. C. Chu for guiding us throughout the project with inspiring advices; and towards Mr. Leon H. S. Chan for helping us out on the technical problems regarding computation and the simulation model, together with some interesting insights on the project. We would also like to thank Mr. W. C. Chan for being the project partner to help us out and cross-check our results. WENO code as our simulation model is a powerful tool and we are glad to thank Mr. Leon H. S. Chan for the modifications and fellow producers Shu (2003).

REFERENCES

Chavanis, P.-H. 2020, arXiv: General Relativity and Quantum Cosmology

D'Amico, G., Kamionkowski, M., & Sigurdson, K. 2009, Dark Matter Astrophysics, arXiv, doi: 10.48550/ARXIV.0907.1912

Dufour, P., Blouin, S., Coutu, S., et al. 2017, in Astronomical Society of the Pacific Conference Series, Vol. 509, 20th European White Dwarf Workshop, ed. P. E. Tremblay, B. Gaensicke, & T. Marsh, 3. https://arxiv.org/abs/1610.00986

Kagan, Y., Surkov, E. L., & Shlyapnikov, G. V. 1997, Phys. Rev. Lett., 79, 2604, doi: 10.1103/PhysRevLett.79.2604

Leung, S.-C., Chu, M.-C., Lin, L.-M., & Wong, K.-W. 2013, Phys. Rev. D, 87, 123506, doi: 10.1103/PhysRevD.87.123506

Oppenheimer, J. R., & Volkoff, G. M. 1939, Phys. Rev., 55, 374, doi: 10.1103/PhysRev.55.374

Peter, A. H. G. 2012, Dark Matter: A Brief Review, arXiv, doi: 10.48550/ARXIV.1201.3942

Santos, L., & Shlyapnikov, G. V. 2002, Phys. Rev. A, 66, 011602, doi: 10.1103/PhysRevA.66.011602

Shu, C.-W. 2003, International Journal of Computational Fluid Dynamics, 17, 107, doi: 10.1080/1061856031000104851